as AP-1 (Wasylyk *et al.*, 1990; Pankov *et al.*, 1994), Sp-1 (Seth *et al.*, 1993), and c-myb (Dudek *et al.*, 1992) has been reported. In addition, DNA-binding motifs, that is, AP2, CEBP, GRE, E-box, CREB, AP-1, and SP-1, correlate with enhanced ets activity (Edelman *et al.*, 2000). As the recognition sequence of SP-1 is located only 30-bp upstream of the ets site in the Id2 promoter, it is suggested that the EWS/ets chimeric proteins may cooperate with SP-1 to enhance the transcriptional activity of Id2. The cooperative effect of ets and E-box-binding proteins with other transcriptional factors is supposed to be crucial to Id2 transactivation, which subsequently contributes to tumor progression.

The high level of Id2 expression may explain certain characteristics of Ewing sarcoma such as primitive morphological features and expression of neural molecules. Several neural antigens are detectable by immunohistochemical analysis in Ewing sarcoma. However, few muscular antigens are detected (Sugimoto *et al.*, 1997). Id proteins interact with ubiquitous bHLH class A proteins, such as E12 and E47, to block the formation of heterodimers of class A proteins and tissue-specific class B proteins, for example Tal-1 and MyoD (Benezra *et al.*, 1990; Langlands *et al.*, 1997). The Id2 expression induced by the specific chimeric proteins thus prevents expression of muscular phenotypes in the Ewing sarcoma. However, expression of Id2 in neurogenesis and during retinoic acid-induced differentiation of neuroblastoma suggests that Id2 is not a general inhibitor of differentiation in neural cell types (Neuman *et al.*, 1993). The neurogenic potential of Ewing sarcoma may be explained by the gaining of tumorigenicity in the process of neurogenic lineage or by the overexpression of Id2 influencing precursor cells of other lineages toward neural crest and neurogenic fates. The primitive morphological appearance in the Ewing tumor family may be attributed to the high levels of Id2 that interfere with the activities of lineage-specific genes to commit cells to terminal differentiation as shown schematically in Figure 6.

The high levels of Id2 may also explain the high malignancy and poor prognosis of this tumor. Id2 expression reverses the inhibition of cellular proliferation and the block in cell cycle progression because of direct interaction of Id2 with RB via disruption of heterodimerization between Rb and E2F (Lasorella *et al.*, 1996). The RB mutant phenotypes, that is ectopic cellular proliferation, loss of differentiation, and cell death, are reported to manifest through uncontrolled Id2 activity in mice (Lasorella *et al.*, 2000). The oncogenic process of Ewing sarcoma may attribute to the Id2-mediated inhibition of RB that has a tumor suppressive activity in a series of cancers.

c-myc, which functions as an oncogenic molecule and was particularly abundant as shown by the arrays of this study, is directly induced by EWS/ets chimeric oncoproteins (Bailly *et al.*, 1994; Noguera *et al.*, 1992). Id2 expression is transactivated by N-myc and c-myc through direct binding to the Id2 promoter. Id2 is overexpressed in cells carrying extra copies of the N-myc gene in neuroblastoma and mediates signaling by myc proteins (Benezra *et al.*, 1990). Thus, the induction of the Id2 gene seems to be augmented by myc oncoproteins that are upregulated by the EWS/ets chimeric proteins. Although further analyses are required, many essential molecules are involved in tumorigenic process executed by Id2 expression.

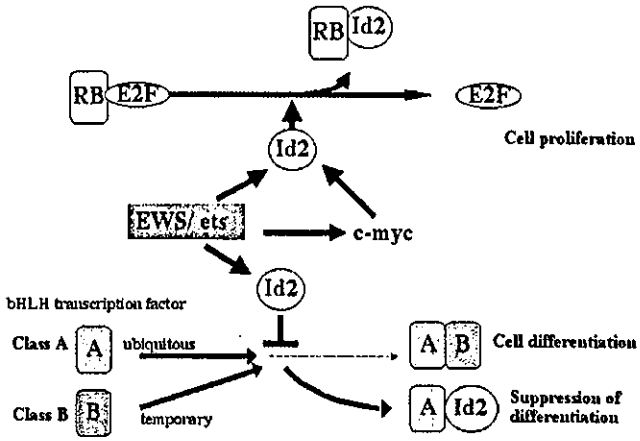

Figure 6 Possible function of EWS/ets chimeric proteins in tumorigenesis. EWS/ets fusion proteins activate the Id2 gene directly, and also indirectly as a result of activating c-myc gene. The higher levels of Id2 protein enhance cell cycle progression by inactivating RB protein family. Id2 protein, furthermore, interferes ubiquitous bHLH class A proteins to form heterodimers with tissue-specific class B proteins, and subsequently inhibits precursor cells to differentiate into a certain lineage

Based on the present experiments, we propose a possible role of EWS/ets chimeric proteins in oncogenesis of Ewing sarcoma (Figure 6). The chimeric proteins directly activate the Id2 gene. Moreover, they induce c-myc expression, with the subsequent high levels of c-myc further augmenting expression of Id2. Consequently, the high levels of Id2 interfere with the growth-suppressive activity of the RB protein family and the differentiation regulated by bHLH transcription factors.

Materials and methods

Cell lines and surgical samples

Surgical samples were obtained from patients with Ewing sarcoma. The cell lines used in this work and the specific fusion transcripts are shown in Table 1. Cells were cultured in RPMI medium supplemented with 10% fetal bovine serum. The surgically resected tumor was immediately frozen in OCT-compound (Miles Inc. Diagnostic Division, Elkhart, IN, USA) for immunohistochemical procedures and for RNA extraction. Diagnosis of Ewing sarcoma was immunohistochemically defined with an anti-p30/32^{MIC2} antibody, and detection of chimeric genes (EWS/Fli-1, EWS/ERG, or EWS/E1AF) was performed by a PCR technique using a specific set of primers described previously (Urano *et al.*, 1998). Neuroblastoma and rhabdomyosarcoma were diagnosed by immunohistological examination. The tumor specimens used in this work, and the specific fusion transcripts of Ewing sarcoma are shown in

Table 1 Cell lines and fusion transcripts

Cell line	*Diagnosis*	*Fusion transcripts*
NCR-EW2	Ewing	EWS exon7/Fli-1 exon 5
NCR-EW3	Ewing	EWS exon7/E1AFexon9
W-ES	Ewing	EWS exon 7/ERG exon 9
SYM-1	Ewing	EWS exon7/Fli-1 exon 5
RD-ES	Ewing	EWS exon7/Fli-1 exon 5
SK- ES1	Ewing	EWS exon7/Fli-1 exon 5
SCCH196	Ewing	EWS exon 7/Fli-1 exon 6
EES-1	Ewing	EWS exon7/Fli-1 exon 6
EW93	Ewing	EWS exon7/Fli-1 exon 6
KU-9	PNET	EWS exon 7/Fli-1 exon 5
PN-1	PNET	not detected
MURAOKA	PNET	EWS exon 10/Fli-1 exon 8
KNB-1	Neuroblastoma	
NCR-G3	Embryonal carcinoma	

PNET: peripheral primitive neuroectodermal tumor.

Table 2 Clinical details of solid tumors

Case	*Age/sex*	*Origin*	*Diagnosis*	*Fusion transcripts*
1	16y/M	Abdomen	Ewing	EWS exon7/Fli-1 exon 7
2	16y/F	Fibula	Ewing	EWS exon 7/Fli-1 exon 5
3	—/M	—	Ewing	EWS exon 7/Fli-1 exon 6
4	26y/M	—	Ewing	EWS exon 7/Fli-1 exon 6
5	—/F	Retroperitoneum	PNET	EWS exon 7/Fli-1 exon 5
6	6y/F	kidney	Ewing	EWS exon 7/Fli-1 exon 5
7	—/M	—	Ewing	EWS exon 7/Fli-1 exon 6
8	17y/F	Adrenal	Ewing	EWS exon 10/Fli-1 exon 8
9	4y/M	Chest wall	Ewing	EWS exon 7/Fli-1 exon 6
7	—/M	—	Ewing	EWS exon 7/Fli-1 exon 6
10	30y/M	Thigh	Ewing	EWS exon 7/Fli-1 exon 5
11	11y/F	Upper limb	Rhabdomyosarcoma	
12	1y/F	Tibia	Rhabdomyosarcoma	
13	1y/F	Neck	Rhabdomyosarcoma	
14	5y/—	Retroperitoneum	Rhabdomyosarcoma	
15	7m/F	—	Neuroblastoma	
16	7m/M	Adrenal	Neuroblastoma	
17	10m/M	—	Neuroblastoma	
18	—/M	—	Neuroblastoma	

M: male, F: female, —: missing data.

Table 2. This work was sanctioned by the Ethics Committee in the Keio University School of Medicine (#13–12).

Gene expression

Isolation of total RNA from Ewing sarcoma cells and tissues was performed using ISOGEN (Nippon Gene Co., Ltd, Tokyo, Japan), and the polyA$^+$ RNA was purified using OligotexTM-dT30 (JSR Corporation, Tokyo, Japan). For investigating differential gene expression, Atlas cDNA Expression Arrays (#7740-1, CLONTECH Laboratories, Inc., CA, USA) were employed. Atlas Arrays were reused three times at most to maintain a high reliability of quantitative analysis. ^{32}P-labeled cDNA probes were generated from each polyA$^+$ RNA sample and hybridized to the Array according to the manufacturer's instructions. The membranes were exposed on an imaging plate and the accumulated radioactivity of each spot was counted with a Bio Imaging Analyzer (BAS-III, Fuji Photo Film Co., Ltd, Tokyo, Japan). The values were normalized by the housekeeping genes spotted on the same membrane. The membrane was also exposed to a Kodak BioMax Ms X-ray film for 1–7 days to obtain a gene expression profile. For Northern blot analysis, 10 μg of each total RNA sample was analyzed as described by Thomas (1980).

Luciferase reporter assay

The activation of the Id2 promoter was examined with a Dual Luciferase Promoter Assay System (Promega, Co., WI, USA). The promoter region was amplified by PCR with the sense and antisense primers, 5′-CCGCACTTACTGTACTGTACTC-3′ and 5′-TGCTGAGCTAGCTGCGCTT-3′, respectively. The PCR product was enzymatically digested with *Rsa* I and *Hae* III, and the 176-bp band from the position −46 to −221 relative to the start site of transcription was ligated into the pGL3-promoter vector. Point mutations were introduced into the promoter sequences of Id2 ligated to the luciferase reporter gene using the Gene Editor *in vitro* Site-Directed Mutagenesis System (Promega). Adenosine at the position −204 relative to

the transcription start site was replaced with thymine (−204A:T), or thymine at −201 was replaced with cytosine (−201T:C) to disrupt the E-box. The guanine at −156 was replaced with thymine (−156G:T), or the adenine at −155 was replaced with cytosine (−155A:C) to disrupt the ets recognition sequence. The sequence of the promoter was confirmed by DNA sequence analysis (MegaBACE 1000, Amersham Pharmacia Biotech, CA, USA). An EWS/Fli-1 expression vector (Type II: EWS exon 7/Fli-1 exon 5) was constructed as follows. A 1771-bp cDNA product was amplified from the NCR-EW2 cell line using PCR primers, sense: 5′-GGAAGGAGAGAAAATGGCGTCC-3′ and antisense: 5′-CTCACAAGATGCTAGGAGACTGAG-3′, and ligated into the pGEM-T-Easy vector. The 1.8-kb fragment from the *Not* I digests of this first vector construct was ligated into the *Not* I site of the expression vector pcDNA3 (Promega). After confirmation of incorporation of the cDNA construct by DNA sequencing, expression was analyzed in HeLa cells by Western blotting. An expression vector of the fusion protein, EWS/Fli-1, EWS/ERG (Ohno *et al.*, 1994) or EWS/EIAF (Urano *et al.*, 1996, 1998) was cotransfected with the luciferase-reporter vector into HeLa cells using Lipofectin Reagent (Life Technologies, MD, USA). The cells were also transfected together with TK-RL reference vector for the standardization of transfection efficiency. The cells were treated according to the directions of the manufacturer. The intensity of the luminescence was measured by a luminometer, GENE LIGHT 55 (Microtec Co., Ltd., Chiba, Japan), and expressed in the ratio of the first luminescence from the reporter gene to the second luminescence from the RL-TK reference gene.

Chromatin immunoprecipitation

The chromatin DNA that interacts with EWS/Fli-1 was detected according to the procedure as described (Moreno *et al.*, 1999) with minor modifications. Briefly, cells fixed with 1% formaldehyde were dispersed in cell lysis buffer [10 mM HEPES pH 7.5, 10 mM EDTA, 0.5 mM EGTA, 0.5% IGEPAL CA-330 (Sigma, St Louis, MO, USA), and Protease Inhibitor Cocktail (Roche Diagnostics GmbH, Mannheim, Germany)]. Nuclei were pelleted, lysed in RIPA buffer (50 mM Tris-HCl pH 7.5, 150 mM NaCl, 1% IGEPAL, 0.1% sodium dodecylsulfate, 0.5% deoxycholate, and Protease Inhibitor Cocktail), sonicated and centrifuged. The supernatant was used as chromatin solution. Anti-Fli-1 antibody (Santa Cruz Biotechnology, Inc., Santa Cruz, CA, USA) or the equivalent amount of rabbit IgG was added and Dynabeads Protein G (Dynal ASA, Oslo, Norway) was employed to precipitate the antigen. The pairs of sense and antisense primers for PCR used to detect the promoter regions were as follows, c-myc: 5′-CATGCGGCTCTCTTACTCTG-3′ and 5′-CGGAGATTAGCGAGAGAGGA-3′; cyclin Dl: 5′-ACTTCGGTGGTCTTGTCCC-3′ and 5′-TCCAGCAGCAGCCCAAGAT-3′; TGF-βIIR: 5′-ACGTCGAGGAGAGGGAGAA-3′ and 5′-AGATGTGCGGGCCAGATGT-3′ ; MMP-1: 5′-GTCTCCTTCGCACAC-3′ and 5′-CTCAGTGCAAGGTAA-3′; EAT/Mcl-1: 5′-TTTGAAAACCTGGGATTGAG-3′ and 5′-GGTCAAATGGAAGGAACTCA-3′; β-actin: 5′-CACCACACTCT-ACCTCTCAAG3′ and 5′-GCCATAAAAGGCAACTTTCGG-3′. The primers for Id2 are stated above.

Acknowledgements

The EWS/ERG expression vector are gifts from T Ohno (Gifu University, School of Medicine). We thank T Fukasawa (Keio University School of Medicine) for reviewing this manuscript, and the staff of Department of Pathology, Keio University School of Medicine for technical assistance. We are grateful to K Saito, S Asai, J Osegawa and K Abe for joining this research as undergraduate students.

This work was partly supported by a Grant-in Aid for Scientific Research from the Ministry of Education, Culture, Sports, Science, and Technology, as well as a Grant-in-Aid for Scientific Research from the Japan Society for the Promotion of Science (JSPS).

References

Bailly RA, Bosselut R, Zucman J, Cormier F, Delattre O, Roussel M, Thomas G and Ghysdael J. (1994). *Mol. Cell Biol.*, **14**, 3230–3241.

Benezra R, Davis RL, Lockshon D, Turner DL and Weintraub H. (1990). *Cell*, **61**, 49–59.

Braun BS, Frieden R, Lessnick SL, May WA and Denny CT. (1995). *Mol. Cell Biol.*, **15**, 4623–4630.

Dauphinot L, De Oliveira C, Melot T, Sevenet N, Thomas V, Weissman BE and Delattre O. (2001). *Oncogene*, **20**, 3258–3265.

Delattre O, Zucman J, Plougastel B, Desmeze C, Melot T, Peter M, Kovar H, Joubert I, de Jong P, Rouleau G, Aurias A and Thomas G. (1992). *Nature*, **359**, 162–165.

Dudek H, Tantravahi RV, Rao VN, Reddy ES and Reddy EP. (1992). *Proc. Natl. Acad. Sci. USA*, **89**, 1291–1295.

Edelman GM, Meech R, Owens GC and Jones FS. (2000). *Proc. Natl. Acad. Sci. USA*, **97**, 3038–3043.

Gegonne A, Bosselut R, Bailly RA and Ghysdael J. (1993). *EMBO J.*, **12**, 1169–1178.

Iavarone A, Garg P, Lasorella A, Hsu J and Israel MA. (1994). *Genes Dev.*, **8**, 1270–1284.

Im YH, Kim HT, Lee C, Poulin D, Welford S, Sorensen PH, Denny CT and Kim SJ. (2000). *Cancer Res.*, **60**, 1536–1540.

Jeon IS, Davis JN, Braun BS, Sublett JE, Roussel MF, Denny CT and Shapiro DN. (1995). *Oncogene*, **10**, 1229–1234.

Langlands K, Yin X, Anand G and Prochownik EV. (1997). *J. Biol. Chem.*, **272**, 19 785–19 793.

Lasorella A, Iavarone A and Israel MA. (1996). *Mol. Cell. Biol.*, **16**, 2570–2578.

Lasorella A, Noseda M, Beyna M, Yokota Y and Iavarone A. (2000). *Nature*, **407**, 592–598.

Martinsen BJ and Bronner-Fraser M. (1998). *Science*, **281**, 988–991.

Matsumoto Y, Tanaka K, Nakatani F, Matsunobu T, Matsuda S and Iwamoto Y (2001). *Br. J. Cancer*, **84**, 768–775.

May WA, Arvand A, Thompson AD, Braun BS, Wright M and Denny CT. (1997). *Nat. Genet.*, **17**, 495–497.

Moreno CS, Beresford GW, Louis-Plence P, Morris AC and Boss JM. (1999). *Immunity*, **10**, 143–151.

Nelsen B, Tian G, Erman B, Gregoire J, Maki R, Graves B and Sen R. (1993). *Science*, **261**, 82–86.

Neuman T, Keen A, Zuber MX, Kristjansson GI, Gruss P and Nornes HO. (1993). *Dev Biol*, **160**, 186–195.

Noguera R, Triche TJ, Navarro S, Tsokos M and Llombart BA. (1992). *Lab. Invest.*, **66**, 143–151.

Norton JD, Deed RW, Craggs G and Sablitzky F. (1998). *Trends Cell Biol.*, **8**, 58–65.
Ohno T, Ouchida M, Lee L, Gatalica Z, Rao VN and Reddy ES. (1994). *Oncogene*, **9**, 3087–3097.
Pankov R, Neznanov N, Umezawa A and Oshima RG. (1994). *Mol. Cell Biol.*, **14**, 7744–7757.
Paulussen M, Ahrens S, Dunst J, Winkelmann W, Exner GU, Kotz R, Amann G, Dockhorn-Dworniczak B, Harms D, Muller-Weihrich S, Welte K, Kornhuber B, Janka-Schaub G, Gobel U, Treuner J, Voute PA, Zoubek A, Gadner H and Jurgens H. (2001). *J. Clin. Oncol.*, **19**, 1818–1829.
Peter M, Couturier J, Pacquement H, Michon J, Thomas G, Magdelenat H and Delattre O. (1997). *Oncogene*, **14**, 1159–1164.
Petermann R, Mossier BM, Aryee DN, Khazak V, Golemis EA and Kovar H. (1998). *Oncogene*, **17**, 603–610.
Seth A, Hodge DR, Thompson DM, Robinson L, Panayiotakis A, Watson OK and Papas TS. (1993). *AIDS Res. Hum. Retroviruses*, **9**, 1017–1023.
Sorensen PH, Lessnick SL, Lopez-Terrada D, Liu XF, Triche TJ and Denny CT. (1994). *Nat. Genet.*, **6**, 146–151.
Sugimoto T, Umezawa A and Hata J. (1997). *Virchows Arch*, **430**, 41–46.
Thomas PS. (1980). *Proc. Natl. Acad. Sci. USA*, **77**, 5201–5205.
Thompson AD, Braun BS, Arvand A, Stewart SD, May WA, Chen E, Korenberg J and Denny C. (1996). *Oncogene*, **13**, 2649–2658.
Toretsky JA, Kalebic T, Blakesley V, LeRoith D and Helman LJ. (1997). *J. Biol. Chem.*, **272**, 30 822–30 827.
Urano F, Umezawa A, Hong W, Kikuchi H and Hata J. (1996). *Biochem. Biophy. Res. Commun.*, **219**, 608–612.
Urano F, Umezawa A, Yabe H, Hong W, Yoshida K, Fujinaga K and Hata J. (1998). *Jpn. J. Cancer Res.*, **89**, 703–711.
Wasylyk B, Wasylyk C, Flores P, Begue A, Leprince D and Stehelin D. (1990). *Nature*, **346**, 191–193.
Yokota Y, Mansouri A, Mori S, Sugawara S, Adachi S, Nishikawa S and Gruss P. (1999). *Nature*, **397**, 702–706.

JOURNAL OF CELLULAR PHYSIOLOGY 194:45–53 (2002)

Use of Isolated Mature Osteoblasts in Abundance Acts as Desired-Shaped Bone Regeneration in Combination With a Modified Poly-DL-Lactic-Co-Glycolic Acid (PLGA)-Collagen Sponge

KENSUKE OCHI,[1,2] GOUPING CHEN,[3] TAKASHI USHIDA,[4] SATOSHI GOJO,[5] KAORU SEGAWA,[6] HITOSHI TAI,[7] KENJU UENO,[7] HIROYUKI OHKAWA,[8] TAISUKE MORI,[1] AKIRA YAMAGUCHI,[9] YOSHIAKI TOYAMA,[2] JUN-ICHI HATA,[1] AND AKIHIRO UMEZAWA[1]*

[1]*Department of Pathology, Keio University School of Medicine, Tokyo, Japan*
[2]*Department of Orthopaedics, Keio University School of Medicine, Tokyo, Japan*
[3]*Tissue Engineering Research Center, AIST, Amagasaki, Japan*
[4]*Biomedical Engineering Laboratory, Graduate School of Engineering, University of Tokyo, Tokyo, Japan*
[5]*Department of Cardiac Surgery, Saitama Medical Center, Saitama, Japan*
[6]*Department of Microbiology, Keio University School of Medicine, Tokyo, Japan*
[7]*Fuji-Gotemba Research Laboratories, Chugai Pharmaceutical Co., Ltd., Shizuoka, Japan*
[8]*Product Research Lab., Chugai Pharmaceutical Co., Ltd., Tokyo, Japan*
[9]*Division of Oral Pathology and Bone Metabolism, Nagasaki University Graduate School of Biomedical Sciences, Nagasaki, Japan*

Controlled regeneration of bone or cartilage has recently begun to facilitate a host of novel clinical treatments. An osteoblast line, which we isolated is able to form new bone matrix in vivo within 2 days and exhibits a mature osteoblast phenotype both in vitro and in vivo. Using these cells, we show that cuboidal bones can be generated into a predesigned shaped-bone with high-density bone trabeculae when used in combination with a modified poly-DL-lactic-co-glycolic acid (PLGA)-collagen sponge. PLGA coated with collagen gel serves as a good scaffold for osteoblasts. These results indicate that mature osteoblasts, in combination with a scaffold such as PLGA-collagen sponge, show promise for use in a custom-shaped bone regeneration tool for both basic research into osteogenesis and for development of therapeutic applications. J. Cell. Physiol. 194: 45–53, 2002.

The concept of regenerative medicine refers to the cell-mediated restoration of damaged or diseased tissue, and practically, regeneration of bone and cartilage may be one of the most accessible approaches. Candidate cell sources for regeneration of tissue include embryonic stem cells, fetal cells or adult cells such as marrow stromal cells (Bianco and Robey, 2000), each of which has both benefits and drawbacks.

Multipotent mesenchymal stem cells have recently been isolated from adult marrow and were shown to proliferate extensively, and to maintain the ability to differentiate into multiple cell types such as osteoblasts, chondrocytes, and myoblasts in vitro (Umezawa et al., 1992; Pittenger et al., 1999; Bianco and Robey, 2000). We have also shown that stromal cells are able to generate cardiomyocytes and endothelial cells (Makino et al., 1999), neuronal cells (Kohyama et al., 2001), and adipocytes (Umezawa et al., 1991). Clinical trials have already been performed using marrow stromal cells to treat patients with osteogenesis imperfecta (Horwitz et al., 1999) and osteoporosis (Canalis, 2000; Rodan and Martin, 2000). Thus, marrow stromal cells are expected to be a good source of cell therapy in addition to embryonic stem cells and fetal cells (Pittenger et al., 2000).

Humoral factors have also been used to induce bone formation (Yamaguchi et al., 2000). Bone morphogenetic proteins (BMPs) such as BMP-7 and BMP-2 induce osteogenesis in vivo when added them to matrix implants (Service, 2000). Treatment of simple collagen matrices with BMPs prompted rapid healing of bone defects in animal models. In human, implants of a

Contract grant sponsor: Ministry of Education, Culture, Sports, Science, and Technology; Contract grant numbers: 11557021, 13470053, 13022264, 11167274; Contract grant sponsor: Keio University Special Grant-in-Aid for Innovative Collaborative Research Project; Contract grant sponsor: National Grant-in-Aid for the Establishment of a High-Tech Research Center at Private Universities.

*Correspondence to: Akihiro Umezawa, Department of Pathology, Keio University, School of Medicine, 35 Shinanomachi, Shinjuku-ku, Tokyo, 160-8582, Japan.
E-mail: umezawa@1985.jukuin.keio.ac.jp

Received 10 April 2002; Accepted 1 August 2002

Published online in Wiley InterScience (www.interscience.wiley.com.), 26 September 2002.
DOI: 10.1002/jcp.10185

collagen matrix with BMP-2 and BMP-7 generate new bone as well as, or better than, autografts of healthy bone transplanted from another part of the patient's body. However, extremely high quantities of BMPs are needed to produce bone matrix, which is a major limitation to this approach (Service, 2000).

A third element required for in vivo bone formation, in addition to stem cells and cytokines, is a matrix or scaffold (Chen et al., 2000a,b). In an attempt to use the stromal system to direct clinical osteogenesis, marrow stromal cells implanted on gelatin sponges were shown to repair a craniofacial defect (Krebsbach et al., 1998; Tabata et al., 2000). Stromal cells implanted on hydorxyapatite/tricalcium phosphate ceramics also regenerated a critical size defect in the tibia, and resulted in consistent bone formation (Krebsbach et al., 1997). Various types of biomaterials as a scaffold is necessary for the successful tissue engineering (Ohgushi and Caplan, 1999).

In the present study, we show that clonal stromal cells can generate bone of custom-shapes and sizes in combination with an appropriate scaffold, in this case poly-DL-lactic-co-glycolic acid (PLGA)-collagen sponge.

MATERIALS AND METHODS

Cell culture

Primary culture of the marrow cells was performed according to Dexter's method (Dexter et al., 1977). Female C3H/He mice (n = 10) were anesthetized with ether, femurs were excised, and bone marrow cells were obtained for primary bone marrow cultures. Cells were cultured in Iscove's modified Dulbecco's medium (IMDM) supplemented with 20% fetal bovine serum (FBS) and penicillin (100 μg/ml)/streptomycin (250 ng/ml) at 37°C in humid air with 5% CO_2. Immortalized cells were obtained by frequent subculture for more than a year. Cell lines from different dishes were subcloned by limiting dilution. The screened line named KUSA/A1 was cultured in the maintenance medium consisting of IMDM supplemented with 10% FBS and penicillin (100 μg/ml)/streptomycin (250 ng/ml) at 37°C in humid air with 5% CO_2 as previously described (Umezawa et al., 1992). As for monolayer culture, KUSA/A1 cells was cultured with 50 μg/ml ascorbic acid and 10 mM sodium β-glycerophosphate in their culture media.

In vitro calcification assay and osteocalcin production

Cells were sonicated in the homogenization-buffer [20 mM Tris/HCl (pH 7.2), 0.1% Triton X-100] after washing twice with PBS. Calcium content in the culture was determined by CalciumC Test (Wako Chemical Co., Japan) according to the manufacturer's suggestion. The amount of osteocalcin into the culture media was determined by RIA using a mouse osteocalcin assay kit (Biomedical Technologies Inc., Stoughton, MA).

Measurement of alkaline phosphatase (ALP) and evaluation of parathyroid hormone (PTH) response

KUSA/A1 cells were analyzed by ALP assay as described (Leboy et al., 1991). PTH response was evaluated in KUSA/A1 cells as described (Sato et al., 1987).

Cytochemical and histochemical staining for ALP activity and β-galactosidase

Cells in 35 mm dishes were maintained in the standard media described above. Fixed cultures and sections were stained for 30 min at 37°C using naphthol AS-MX phosphate as a substrate and fast red violet LB salt as a coupler. Some cultures were maintained with standard media supplemented with 50 μg/ml ascorbic acid and 10 mM sodium β-glycerophosphate for up to 30 days in vitro. Sections were also stained with Xgal for 8 h at 37°C. Cells expressing β-galactosidase show a blue color after incubation with the Xgal substrate. In our hands, color formation was evident by 10–30 min incubation.

RNA extraction and Northern blotting

RNA was prepared by homogenizing the specimens in guanidinium isothiocyanate followed by centrifugation over a cesium chloride cushion as previously described (Umezawa et al., 1991). The RNA was then electrophoresed in a 1.0% agarose gel, transferred to a nylon filter (NEN Research Products, Boston MA), and hybridized with a murine collagen α2(I) (TIE5) cDNA probe (Amagai et al., 1989). The probe was labeled with [α-^{32}P]-CTP by the random-primer method (Feinberg and Vogelstein, 1983). Hybridization was carried out at 65°C for 14–16 h in a buffer containing five times SSPE (one time SSPE is 0.18 M NaCl, 10 mM NaH_2PO4/Na_2HPO_4 <pH 7.0>, pH 7.4, 1 mM EDTA), five times Denhardt's solution (one time Denhardt's solution is 0.02% Ficoll, 0.02% polyvinylpyrrolidone, 0.02% bovine serum albumin), 0.02% poly A, and 1% sodium dodecyl sulfate (SDS). The blots were washed with one time SSC containing 1% SDS at 65°C. The blots were exposed to X-ray film at −80°C using an intensifying screen.

Three dimensional collagen gel culture

KUSA/A1 cells were dispersely embedded in type I collagen gels. Eight volumes of cooled collagen solution (I-A Cellmatrix, Nitta gelatin, Osaka, Japan), one volumes of ten times concentrated IMDM medium, and one volume of buffer solution (0.05 N NaOH containing 2.2% $NaHCO_3$ and 200 mM HEPES) were added with gentle shaking on ice to ten volumes of IMDM medium suspension containing 10^7 cells/ml KUSA/A1 cells. Two hundred microliters of this medium-cell-collagen mixture was placed in each well of 96 well plastic microwell plate and allowed to gel by incubation at 37°C for 30 min. The gels were transferred to a 10 mm plastic dish and overlaid with 10 ml of IMDM containing 10% FBS. Cell cultures were incubated in 5% CO_2 at 37°C and the medium was changed every 3 days.

Introduction of the β-galactosidase gene

Recombinant adenovirus expressing bacterial β-galactosidase was prepared as described (Yamashita et al., 1999). Cells were infected by this virus at 10 plaque forming unit/cell. The expression of the β-galactosidase gene in KUSA/A1 was determined cytochemically in vitro. Nearly all the cells expressed β-galactosidase 3 days after transfection.

Inoculating of cells into syngeneic mice

Culture medium containing either KUSA/A1 cells (10^7 cells/ml) was injected to 8–12 weeks old female

C3H/He mice subcutaneously. The tumors were harvested and fixed in 20% formalin 1 day to 8 weeks after the inoculation. Serial paraffin sections were prepared and stained with either hematoxylin and eosin (H&E), von Kossa or Toluidine Blue stain.

In vivo culture in diffusion chamber

Paired diffusion chambers were constructed using lucid rings and 0.45 μm membrane filters (Millipore Corporation, Bedford, MA) (Urist et al., 1982). The chambers shared a common filter. One chamber contained either KUSA/A1 cells in 200 μl aliquots from six dishes of confluent cultures. After receiving the contents, chambers were implanted subcutaneously in 8–12 weeks old female C3H/He mice. The animals were sacrificed after 2–8 weeks. The chambers were fixed in 20% formalin. Serial paraffin sections were prepared and stained with either hematoxylin and eosin, von Kossa or Toluidine Blue stain.

Preparation of cells, staining procedures, and fluorescence activated cell analysis

All samples (KUSA/A1) were treated by water lysis. Cells, at a final concentration of 1×10^7/ml, were incubated with 1 μg/μl monoclonal antibodies in Hank's balanced salt solution (containing 0.1% albumin and 0.1% sodium azide). In case that the first antibody is conjugated with biotin, cells were washed twice and incubated with streptoavidin-phycoerythrin (Gibco-BRL, Rockville, MD) for 30 min on ice. Purified antibodies in the first step were stained with FITC conjugated goat anti-mouse antibody. Antibodies (anti-mouse Flk-1, CD31, CD34, c-kit, Sca-1, CD140a, CD144, CD14, CD29, CD41, CD44, CD49b, CD49d, CD54, CD90, CD102, CD106, Ly-6C and Ly-6G, and isotype control antibodies) were purchased from Pharmingen Pharmaceutical, Inc. (San Diego, CA). After two washes with Hank's balanced salt solution, propidium iodide (PI) was added to each test tube at a concentration of 1 mg/ml just before acquisition by FACScan flow cytometry (Beckton Dickinson, Franklin Lakes, NJ) with the Argon laser at 488 nm. List mode data for 30,000–50,000 cells were collected in PI gate.

PLGA-collagen hybrid sponge preparation

Biodegradable hybrid sponge of PLGA (a 75:25 copolymer of lactic acid and glycolic acid with molecular weight of 90–126 kDa) and collagen was used as the three-dimensional porous scaffold for implantation (Chen et al., 2000a,b). The hybrid sponge was prepared by forming microsponges of collagen in the pores of PLGA sponge. At first, a PLGA sponge was prepared by a particulate-leaching technique using sieved sodium chloride particulates. PLGA polymer was dissolved in chloroform to prepare a PLGA solution in chloroform at a concentration of 20% (w/v). Sieved NaCl particulates (9.0 g), ranging in diameter from 355 to 425 μm, were added to the PLGA solution (5 ml), vortexed, and poured into an aluminum pan. The chloroform was allowed to evaporate by air-drying in a draft for 24 h and followed by 24 h of vacuum drying. The PLGA sponge with porosity of 90% and pore size of 355–425 μm was formed after NaCl particulates were leached out by washing with deionized water. Subsequently, the PLGA sponge was immersed in a bovine collagen acidic solution (type I, pH 3.2, 5 μg/μl) under a vacuum so that the sponge pores filled with collagen solution. The collagen solution containing PLGA sponge was then frozen at −80°C for 12 h and lyophilized under a vacuum of 0.2 Torr for an additional 24 h to allow the formation of collagen microsponges in the sponge pores. Finally, the collagen microsponges were cross-linked by treatment with glutaraldehyde vapor saturated with 25% glutaraldehyde aqueous solution at 37°C for 4 h; and non-reacting aldehyde groups were blocked by treating with 0.1 M glycine aqueous solution. After washing with deionized water and lyophilizing, the PLGA-collagen hybrid sponge was prepared. The formation of collagen microsponge in the pores of PLGA sponge was confirmed by SEM observation. The hybrid sponge was sterilized using ethylene oxide.

Transplantation of cells in the PLGA sponge

KUSA/A1 suspension (10^7/ml) was injected gently into PLGA sponges. After injection, the sponges were incubated at 37°C for more than 30 min. Then the sponges were transplanted into subcutaneous tissue or abdominal cavity of mice. These operation plans are accepted by the Laboratory animal care and use committee of Keio University School of Medicine (#000024). All the experiments were followed by the guideline for the care and use of laboratory animals of Keio University School of Medicine.

RESULTS

Characterization of isolated differentiated osteoblasts

KUSA/A1 cells were originally isolated as cells which induce hematopoiesis in vivo (Umezawa et al., 1992). When cultured in monolayer, the cells were spindle-shaped in the growth phase and after confluence (Fig. 1A,B). Extracellular matrix positive for von Kossa stain appeared in cell culture and increased after confluence (Fig. 1C,D). Ultrastructurally, the matrix was electron dense and was clearly produced by the cells (Fig. 1E). RNA blot hybridization showed that the collagen α2(I) gene was expressed at a high level in KUSA/A1 cells, the same as in other stromal cell lines (Fig. 1F) (Umezawa et al., 1992).

We analyzed growth curve, ALP activity, in vitro calcification, osteocalcin (bone gla protein) release, and response to PTH in comparison with MC3T3-E1 cells. KUSA/A1 proliferation, which was measured by DNA content, was equivalent to that of MC3T3-E1 cells. ALP activity of KUSA/A1 cells in growth phase was approximately tenfold higher than in MC3T3-E1 cells (Fig. 1G). In vitro calcification, which steadily increased both before and after confluence, was approximately 100-fold higher after the confluent stage in KUSA/A1 cells than in MC3T3-E1 cells (Fig. 1H). Osteocalcin release into culture media peaked on day 5 in KUSA/A1 cells and was two- to threefold higher than in MC3T3-E1 cells (Fig. 1I). PTH response, measured as cAMP production, gradually decreased during the culture period in KUSA/A1 cells but increased in MC3T3-E1 cells (Fig. 1J). This response to PTH did not require any induction and was independent of culture conditions.

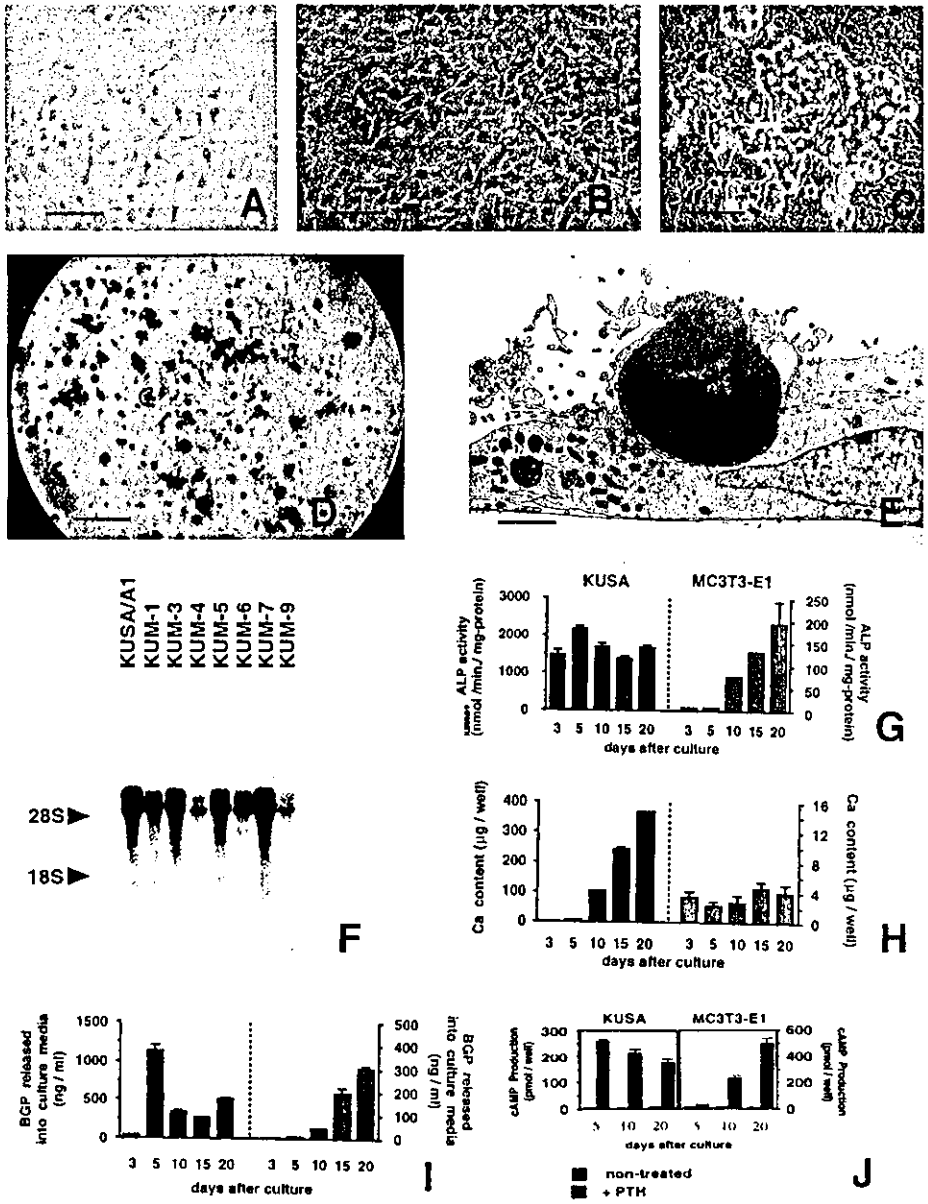

Fig. 1. In vitro characteristics of KUSA/A1 cells as a mature osteoblast model. **A**: Phase contrast micrograph of KUSA/A1 cells at the semiconfluent stage. **B**: KUSA/A1 cells 7 days postconfluence. **C**: Extracellular matrix produced from KUSA/A1 cells. **D**: Calcium deposition in KUSA/A1 culture. KUSA/A1 cells cultured in supplemented medium containing β-glycerophosphate were fixed and stained in situ by the von Kossa technique. **E**: Transmission electron micrograph of the extracellular matrix produced by KUSA/A1. **F**: Expression of the collagen α2(I) gene in marrow stromal cell lines (Umezawa et al., 1992). **G**: ALP activity in KUSA/A1 cells and MC3T3-E1 cells. **H**: Quantitative analysis of calcium deposition in KUSA/A1 cells and MC3T3-E1 cells. **I**: Bone Gla protein (osteocalcin) secretion in KUSA/A1 cells and MC3T3-E1 cells. **J**: cAMP production after PTH treatment. PTH response of KUSA/A1 cells was compared with that of MC3T3-E1 cells, as measured by cAMP production. Scale bars: 120 μm (A,B,C), 5 mm (D), 2 μm (E).

Three-dimensional culture of KUSA/A1 cells in collagen gels

To generate a three-dimensional cell culture system, KUSA/A1 cells were suspended and cultured in collagen gels (Fig. 2). Gels containing KUSA/A1 were transparent in vitro under a phase contrast microscopy on day 3 and remained semi-transparent until 2 weeks. Histologically, KUSA/A1 cells formed a reticular network, which had evidence of calcification by von Kossa staining at 2 weeks. These cells exhibited high ALP activity. At 4 weeks, heavy calcium deposition had rendered the gels opaque, even though the cultures were not supplemented with β-glycerophosphate.

In vivo osteogenic activity in KUSA/A1 cells

To determine the potential osteogenic activity of KUSA/A1 in vivo, the cells were injected subcutaneously into syngeneic mice (Fig. 3A–E). Before inoculation,

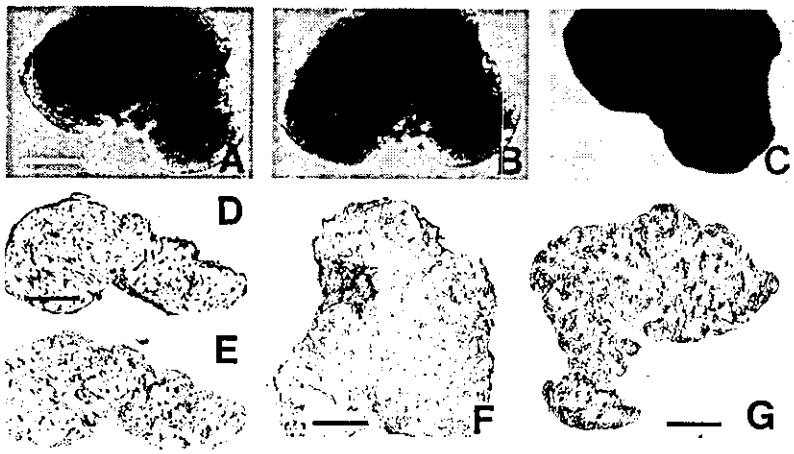

Fig. 2. Three-dimensional culture of KUSA/A1 cells in collagen gel. Phase contrast micrograph of three-dimensional culture of KUSA/A1 cells in collagen gel for 3 days (**A**), 2 (**B**), and 4 weeks (**C**). At 4 weeks, gels have become opaque. **D**: Microscopic examination of KUSA/A1 in collagen gels at 2 weeks. H&E stain. KUSA/A1 cells connected with each other and formed a reticular network. **E**: KUSA/A1 culture in collagen gels with von Kossa staining. The cells were cultured without β-glycerophosphate. **F**: ALP cytochemical staining of KUSA/A1 cells at 2 weeks. **G**: von Kossa staining of KUSA/A1 culture at 4 weeks. Scale bars: 170 μm (A,D,F,G).

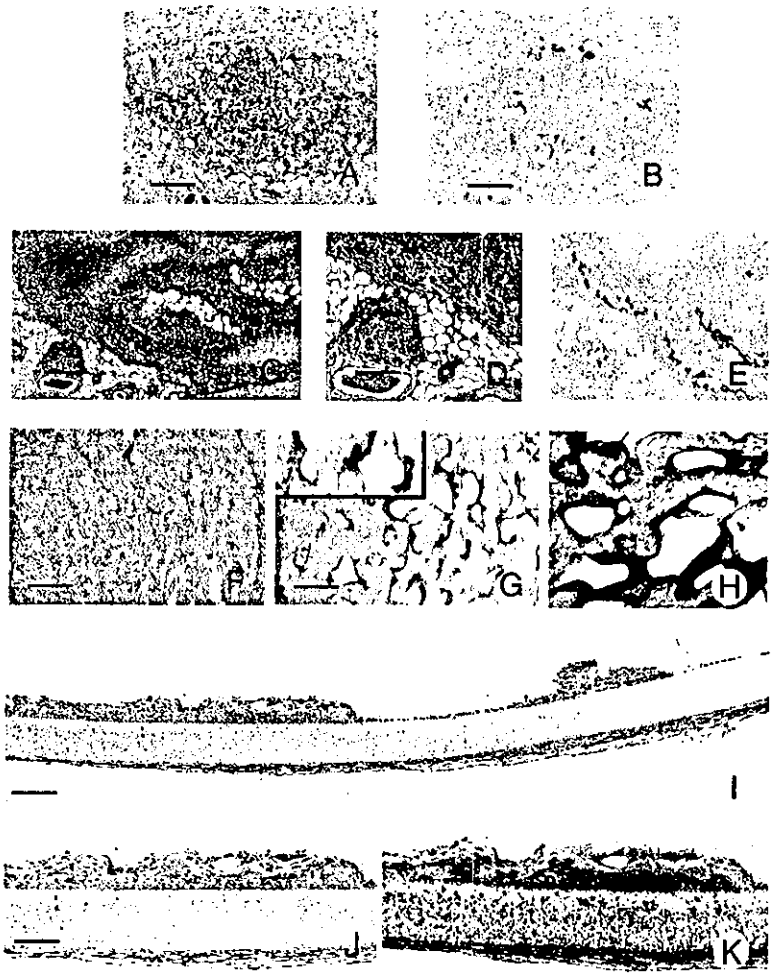

Fig. 3. Membranous ossification by KUSA/A1 in vivo. **A** and **B**: Microscopic examination of KUSA/A1 tumor in the subcutaneous tissue 2 days after injection. H&E stain (A) and von Kossa stain (B). Bone matrix was detected on day 2. **C**: KUSA/A1 tumor on day 3. H&E stain. **D**: Higher magnification of C. **E**: KUSA/A1 tumor on day 3 stained with von Kossa stain. Bone matrix had increased on day 3, as compared with day 2. **F**: Complete bone formation with a marrow cavity at 8 weeks. **G**: Enzyme histochemistry for β-galactosidase of KUSA/A1 tumor, 2 weeks after inoculation. Bone was generated by KUSA/A1 cells, which were transfected with β-galactosidase. **H**: Enzyme histochemistry for ALP of KUSA/A1 tumor, 2 weeks after injection. KUSA/A1 cells, which induce bone, were strongly positive for ALP. **I**, **J**, and **K**: In vivo diffusion chamber analysis of KUSA/A1 cells. Bone formation was detected not only inside the chamber but also outside the chamber, 4 weeks after transplantation. Note that calcium deposition was also observed outside the membrane as well as inside the membrane. I and J: H&E stain. K: von Kossa stain. Scale bars: 160 (A and B), 340 (C), 160 (D), 340 (E), 400 (F), 290 (G), 150 (G, inlet), 60 (H), 90 (I), 140 μm (J and K).

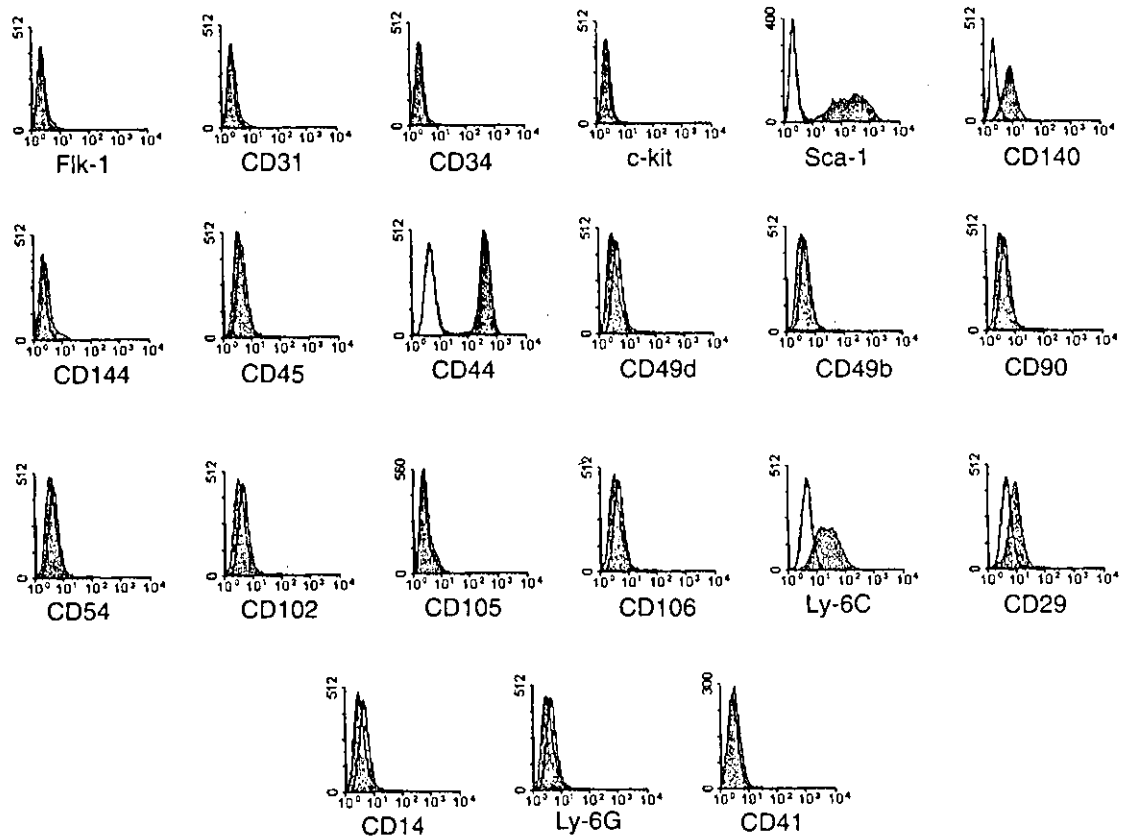

Fig. 4. Flow cytometry analysis of cell surface markers in KUSA/A1 cells. Cells stained with primary antibodies to Flk-1, CD31, CD34, c-kit, Sca-1, CD140, CD144, CD45, CD44, CD49d, CD49b, CD90, CD54, CD102, CD105, CD106, Ly-6C, CD29, CD14, Ly-6G, and CD41, are shown as gray peaks. The isotope controls are shown as white peaks.

cells were cultured for more than 5 days postconfluence. The inoculated cells were negative for calcium deposition on day 1 after the inoculation. But, bone matrix positive for von Kossa stain appeared in the injected cells on day 2, and had markedly increased and become larger, and the matrix became strongly positive for von Kossa stain on day 3. Marrow cavities were formed inside the bone generated by KUSA/A1 cells at 8 weeks and at later stages after inoculation. Hematopoietic cells were also observed in these bone marrow, as reported previously (Umezawa et al., 1992). No cartilage was formed in any KUSA/A1-transplanted bones, indicating that osteogenesis by KUSA/A1 is membranous ossification rather than enchondral ossification.

We continued to observe the fate of KUSA/A1 bone transplanted into the subcutaneous tissue and abdominal cavity, and found that the ectopic KUSA/A1 bone remained unchanged in size and shape for 12 months at both sites. Histologically, complete functional hematopoiesis by ectopic KUSA/A1 bone was seen in the subcutaneous tissue but not in the abdominal cavity.

Osteogenesis was directly generated by the inoculated KUSA/A1 osteoblasts

To determine whether these bones were directly formed by KUSA/A1 cells or generated by host-derived cells, we labeled KUSA/A1 cells with bacteria-derived β-galactosidase (Fig. 3F–H). Frozen tissue sections showed that osteoblasts in the bone were positive for β-galactosidase. The osteoblastic cells, which exhibited strong β-galactosidase activities were also strongly positive for ALP. Sarcomatous proliferation of the inoculated cells, which were positive for β-galactosidase was not seen around the generated bone.

We also injected KUSA/A1 cells into a diffusion chamber and examined osteogenesis (Fig. 3I–K). This was performed to determine whether these bones were directly formed by KUSA/A1 cells or generated by host-derived cells, and whether osteogenesis requires direct cell–cell interactions with the adjacent cells. Diffusion chambers containing KUSA/A1 cells were transplanted subcutaneously into mice. Bone was formed inside the chamber 2 weeks after the transplantation and had calcium deposition. This bone formation became more evident from 4 weeks after the inoculation. Surprisingly, we observed bone formation even outside the chamber in specimens taken at 4 weeks. Calcification was also seen both inside and outside the chamber, suggesting that remarkably strong osteogenic soluble factors or cytokines were being secreted from KUSA/A1 cells. Interestingly, calcium deposition was also reproducibly detected in the membrane. Therefore, osteogenesis is induced directly by KUSA/A1 cells rather than indirectly by neighboring cells.

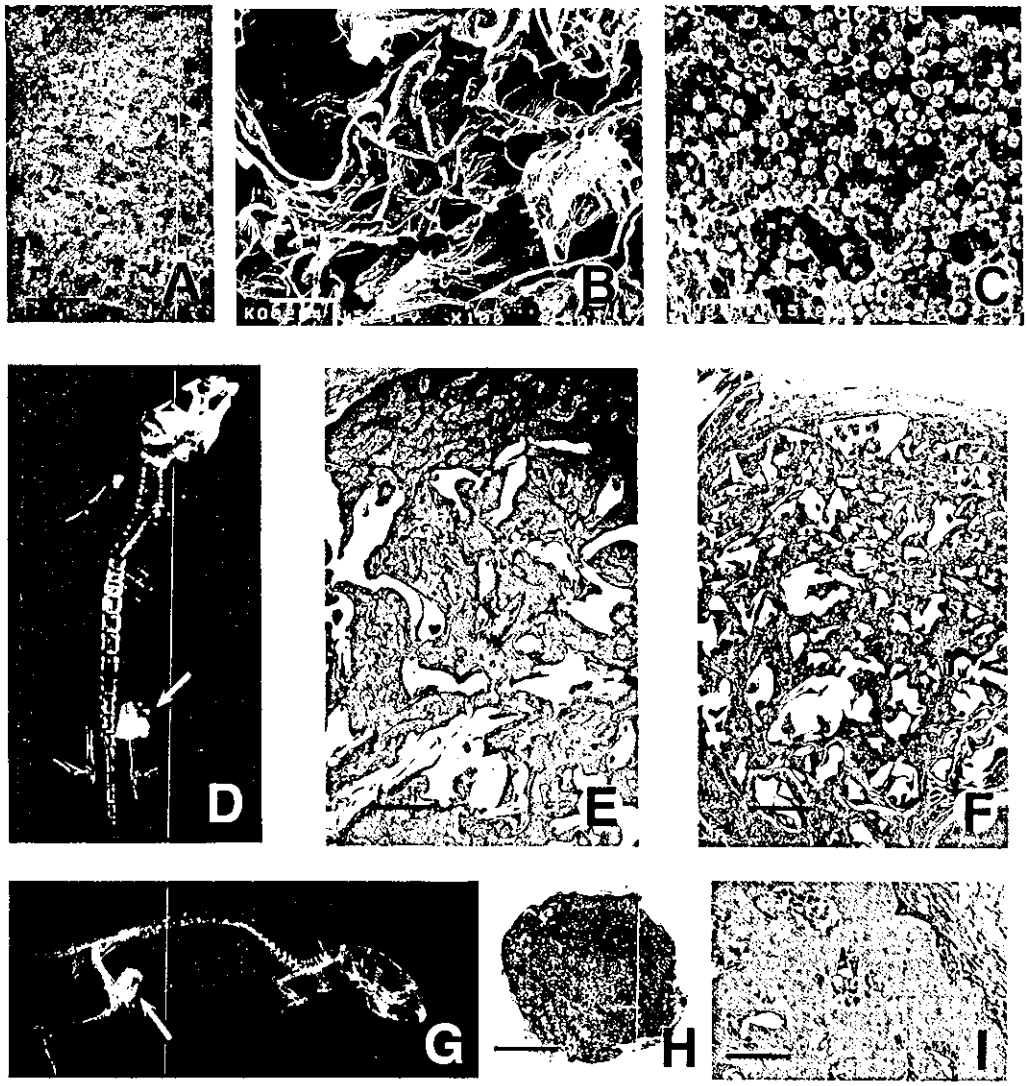

Fig. 5. Generation of custom-shaped bone by KUSA/A1 cells with PLGA-collagen sponge. PLGA-collagen sponge was used as a scaffold for KUSA/A1 cells. **A**: Macroscopic view of PLGA-collagen sponge. **B**: SEM of surface morphology of PLGA-collagen sponge without cells. **C**: SEM of PLGA-collagen sponge, into which KUSA/A1 cells were implanted. PLGA-collagen sponge, into which KUSA/A1 cells were implanted, was transplanted into the syngeneic mice. Six (**D–F**) or 11 (**G–I**) weeks after the transplantation, the KUSA/A1 in the sponge was excised for analysis. D: Soft X-ray of KUSA/A1 bone that is seen as an electron-dense, cuboidal bone. E: Histological examination of the bone generated by KUSA/A1 and PLGA-collagen sponge. Bone trabeculae were clearly seen. F: Histological examination of transplanted PLGA-collagen sponge without cells. Note that foreign body reaction was seen inside the transplanted sponge, but no bone was formed. G: Photo for soft X-ray of complete cuboidal bone by KUSA/A1 and PLGA-collagen sponge. H: Histology of complete cuboidal bone with high density of bone trabeculae. Note that bone was formed even in the center of the sponge. I: High power view of H. Scale bars: 350 (A), 100 (B), 72 (C), 200 μm (E and F), 5 mm (H), 250 μm (I).

Surface marker expression on KUSA/A1 cells

We analyzed the cell surface markers on the clonal KUSA/A1 cells by flow cytometry to better characterize these cells. Cells were incubated with monoclonal antibodies. Controls included cells stained with individual isotype (mouse IgG1 or rat IgG2a). Incubations were performed in the presence of mouse immunoglobulin to prevent nonspecific antibody binding. The cells were found to be strongly positive (more than tenfold greater than the isotype control) for Sca-1, CD44, Ly-6C and CD140, weakly positive for CD29, and negative for c-kit, Flk-1, CD14, CD31, CD34, CD41, CD45, CD49b, CD49d, CD54, CD90, CD102, CD105, CD106, CD144 and Ly-6G (Fig. 4). Surface marker analysis of KUSA/A1 indicated that cells with strong in vivo osteogenic activity exhibited markers for osteocytes (Horowitz et al., 1994; Hughes et al., 1994; Chen et al., 1999); CD44 and Ly-6C. Interestingly, the lack of CD90 expression supported the assumption that these cells maintain a matured phenotype even when they proliferate, since CD90 is detected in the early stage of osteoblast differentiation and declines as osteoblasts mature into osteocytes. Therefore, KUSA/A1 cells, which have strong in vivo osteogenic activity, express markers for mature osteoblasts or osteocytes. This was

confirmed with the cytochemical analysis of KUSA/A1 cells in vivo and in vitro. High ALP activity, calcium deposition, and osteocalcin release with low PTH responsibility also indicate that KUSA/A1 cells are mature osteoblasts or osteocytes.

Generating custom-shaped bones derived from KUSA/A1 cells in vivo with PLGA-collagen sponge

We attempted to generate bone tissue of desired sizes and shapes with a view to future clinical applications (Fig. 5). We previously developed a PLGA-collagen sponge with a pore of specific size for this purpose (Chen et al., 2000a,b). Collagen gels suspended with KUSA/A1 cells were injected into a cube of PLGA-collagen sponge, which was then transplanted into subcutaneous tissue and the abdominal cavity. Two weeks after the transplantation, cuboidal bone was seen on X-ray and formation of bone trabeculae was confirmed histologically. This bone formation was evident at 6 weeks. At 11 weeks, the PLGA sponge turned completely to bone. Hematopoietic cells and tartaric acid-resistant acid phosphatase-positive osteoclasts were also observed in the generated bone. Control PLGA sponges without any cells transplanted into both subcutaneous tissue and abdominal cavity showed no evidence of calcification or ossification.

DISCUSSION

Establishment of rapid and efficient membranous osteogenesis system by mature osteoblasts

We have devised and tested a system for regeneration of bone of specific shape and size that can be successfully implanted into mice using a clonal mature osteoblast cell line. These cells consistently differentiate to form bone both in vitro and in vivo. Very rapid, within 2 days, in vivo bone formation was obtained using mature KUSA/A1 osteoblasts that were cultured for 5–7 days at confluence before implantation. Cells implanted at semiconfluence, in contrast, took 2 weeks to generate bone (Umezawa et al., 1992). Since osteoprogenitor cells divide early in culture and have a limited capacity for self-renewal (McCulloch et al., 1991), these results suggest that use of mature osteoblasts is prerequisite for rapid bone formation in vivo. The in vivo osteogenic activity of the KUSA/A1 cells seems to be at least mediated by humoral factors produced by the cells per se, since bone formed not only inside the diffusion chamber but also outside the chamber, when the cells were transplanted into the chamber.

It would be interesting to assess the possibility of using mature osteoblasts as a therapeutic agent. Injection of isolated mature osteoblasts into a bone defect or fracture site would be more efficient means of accelerating bone fusion with minimal invasion than injection of all types of marrow cells into fracture sites.

PLGA-collagen sponge gave control over the shape and size of osteogenesis

We hypothesized that provision of a scaffold may effectively limit and guide new bone formation. Inoculation of KUSA/A1 cells cultured in collagen gel successfully induced bone in vivo, but collagen gel is too soft to maintain any specific desired shape in vivo, especially at the site of bone defects. However, the PLGA-collagen sponge could both support osteoblast-mediated bone formation and retain its shape in vivo. PLGA-collagen sponge has a number of advantages as a scaffold for bone regeneration: (a) it is easily shaped; (b) the time course of degradation, mechanical strength, and plasticity can be easily modulated by changing the ratio of PLA and PGA; (c) it has a high affinity for cells, mediated by collagen; (d) cells can be injected evenly throughout the sponge so that the sponge turns completely to bone.

In regenerating articular cartilage, it is an important issue how to make mechanically strong, fully weight-bearing cartilage. To this end, subchondral bone, which undercoats cartilage and confers mechanical strength to articular cartilage needs to be generated. Cartilage has been successfully regenerated, however, connection between bone and regenerated cartilage was incomplete. Our present studies suggest that osteoblasts in a scaffold serve a possible candidate for a glue to bind subchondral bone and regenerated cartilage.

Importantly, custom-shaped bone regeneration using mature osteoblasts proved to be successful. Furthermore, transplanted KUSA/A1 cells did not transform into malignant cells, form any abnormal extracellular matrices, or induce any significant inflammatory reactions. The next step will be to isolate human counterparts to these mouse cell lines. Cell separation of osteoblasts from human marrow stroma and inoculation of the cells with appropriate scaffold will provide us a new ways of osteogenesis engineering.

ACKNOWLEDGMENTS

We thank Y. Uchida and S. Higashi for their support and A. Thomson and A. Suzuki for reviewing the manuscript. We also thank S. Kusakari, H. Suzuki, T. Nagai, Y. Hashimoto, T. Inomata, and K. Takeichi for their technical assistance; H. Amano, H. Imabayashi, and K. Watanabe, for discussion; T. Matsumura, H. Okushima and Y. Masaki for encouragement. This work was supported by a grant from the Ministry of Education, Science and Culture to A. U. and J. H., by Keio University Special Grant-in-Aid for Innovative Collaborative Research Project to J. H. and A. U., and by a National Grant-in-Aid for the Establishment of a High-Tech Research Center at Private Universities.

LITERATURE CITED

Amagai M, Inokuchi Y, Nishikawa T, Shimizu Y, Shimizu N. 1989. Cloning of TPA-inducible early (TIE) genes by differential hybridization using TPA-nonresponsive variant of mouse 3T3-L1 cells. Somat Cell Mol Genet 15:153–158.

Bianco P, Robey PG. 2000. Marrow stromal stem cells. J Clin Invest 105:1663–1668.

Canalis E. 2000. Novel treatments for osteoporosis. J Clin Invest 106:177–179.

Chen XD, Qian HY, Neff L, Satomura K, Horowitz MC. 1999. Thy-1 antigen expression by cells in the osteoblast lineage. J Bone Miner Res 14:362–375.

Chen G, Ushida T, Tateishi T. 2000a. A biodegradable hybrid sponge nested with collagen microsponges. J Biomed Mater Res 51:273–279.

Chen G, Ushida T, Tateishi T. 2000b. Hybrid biomaterials for tissue engineering: A preparative method for PLA or PLGA-collagen hybrid sponges. Adv Mater 12:455–457.

Dexter TM, Allen TD, Lajtha LG. 1977. Conditions controlling the proliferation of haemopoietic stem cells in vitro. J Cell Physiol 91: 335–344.

Feinberg AP, Vogelstein B. 1983. A technique for radiolabeling DNA restriction endonuclease fragments to high specific activity. Anal Biochem 132:6–13.

Horowitz MC, Fields A, DeMeo D, Qian HY, Bothwell AL, Trepman E. 1994. Expression and regulation of Ly-6 differentiation antigens by murine osteoblasts. Endocrinology 135:1032–1043.

Horwitz EM, Prockop DJ, Fitzpatrick LA, Koo WW, Gordon PL, Neel M, Sussman M, Orchard P, Marx JC, Pyeritz RE, Brenner MK. 1999. Transplantability and therapeutic effects of bone marrow-derived mesenchymal cells in children with osteogenesis imperfecta. Nat Med 5:309–313.

Hughes DE, Salter DM, Simpson R. 1994. CD44 expression in human bone: A novel marker of osteocytic differentiation. J Bone Miner Res 9:39–44.

Kohyama J, Abe H, Shimazaki T, Koizumi A, Nakashima K, Gojo S, Taga T, Okano H, Hata J, Umezawa A. 2001. Brain from bone: Efficient 'meta-differentiation' of marrow stroma-derived mature osteoblasts to neurons with Noggin or a demethylating agent. Differentiation 68:235–244.

Krebsbach PH, Kuznetsov SA, Satomura K, Emmons RV, Rowe DW, Robey PG. 1997. Bone formation in vivo: Comparison of osteogenesis by transplanted mouse and human marrow stromal fibroblasts. Transplantation 63:1059–1069.

Krebsbach PH, Mankani MH, Satomura K, Kuznetsov SA, Robey PG. 1998. Repair of craniotomy defects using bone marrow stromal cells. Transplantation 66:1272–1278.

Leboy PS, Beresford JN, Devlin C, Owen ME. 1991. Dexamethasone induction of osteoblast mRNAs in rat marrow stromal cell cultures. J Cell Physiol 146:370–378.

Makino S, Fukuda K, Miyoshi S, Konishi F, Kodama H, Pan J, Sano M, Takahashi T, Hori S, Abe H, Hata J, Umezawa A, Ogawa S. 1999. Cardiomyocytes can be generated from marrow stromal cells in vitro. J Clin Invest 103:697–705.

McCulloch CA, Strugurescu M, Hughes F, Melcher AH, Aubin JE. 1991. Osteogenic progenitor cells in rat bone marrow stromal populations exhibit self-renewal in culture. Blood 77:1906–1911.

Ohgushi H, Caplan AI. 1999. Stem cell technology and bioceramics: From cell to gene engineering. J Biomed Mater Res 48:913–927.

Pittenger MF, Mackay AM, Beck SC, Jaiswal RK, Douglas R, Mosca JD, Moorman MA, Simonetti DW, Craig S, Marshak DR. 1999. Multilineage potential of adult human mesenchymal stem cells. Science 284:143–147.

Pittenger MF, Mosca JD, McIntosh KR. 2000. Human mesenchymal stem cells: Progenitor cells for cartilage, bone, fat and stroma. Curr Top Microbiol Immunol 251:3–11.

Rodan GA, Martin TJ. 2000. Therapeutic approaches to bone diseases. Science 289:1508–1514.

Sato K, Han DC, Ozawa M, Fujii Y, Tsushima T, Shizume K. 1987. A highly sensitive bioassay for PTH using ROS 17/2.8 subclonal cells. Acta Endocrinol (Copenh) 116:113–120.

Service RF. 2000. Tissue engineers build new bone. Science 289:1498–1500.

Tabata Y, Hong L, Miyamoto S, Miyao M, Hashimoto N, Ikada Y. 2000. Bone formation at a rabbit skull defect by autologus bone marrow combined with gelatin microspheres containing TGF-beta1. J Biomater Sci Polym Ed 11:891–901.

Umezawa A, Tachibana K, Harigaya K, Kusakari S, Kato S, Watanabe Y, Takano T. 1991. Colony-stimulating factor 1 is downregulatd during the adipocyte differentiation of H-1/A marrow stromal cells and induced by cachectin/tumor necrosis factor. Mol Cell Biol 11:920–927.

Umezawa A, Maruyama T, Segawa K, Shadduck RK, Waheed A, Hata J. 1992. Multipotent marrow stromal cell line is able to induce hematopoiesis in vivo. J Cell Physiol 151:197–205.

Urist MR, Mizutani H, Conover MA, Lietze A, Finerman GA. 1982. Dentin, bone, and osteosarcoma tissue bone morphogenetic proteins. Prog Clin Biol Res 101:61–81.

Yamaguchi A, Komori T, Suda T. 2000. Regulation of osteoblast differentiation mediated by bone morphogenetic proteins, hedgehogs, and Cbfa1. Endocr Rev 21:393–411.

Yamashita T, Tonoki H, Nakata D, Yamano S, Segawa K, Moriuchi T. 1999. Adenovirus type 5 E1A immortalizes primary rat cells expressing wild-type p53. Microbiol Immunol 43:1037–1044.

Pathology International 2003; **53**: 214–220

Original Article

Responsiveness of chemotherapy based on the histological type and Wilms' tumor suppressor gene mutation in bilateral Wilms' tumor

Rie Shibata,[1] Ayako Takata,[1] Akinori Hashiguchi,[1] Akihiro Umezawa,[1] Taketo Yamada[1] and Jun-ichi Hata[1,2]

[1]*Department of Pathology, Keio University School of Medicine, and* [2]*National Research Institute for Child Health and Development, Tokyo, Japan*

To clarify a characteristic of bilateral Wilms' tumor (WT), we examined the clinical and histological features, chemotherapy response and mutations in Wilms' tumor suppressor gene (*WT1*) in five patients. Deoxyribonucleic acid was extracted from peripheral lymphocytes and tumor samples, and direct DNA sequencing was performed to detect *WT1* mutations. Paraffin sections were stained with H&E for histological review and immunostained with anti-*WT1*, anti-Ki-67, anti-S-100 protein and antimyogenin antibodies. In contrast to the single case of epithelial-type WT, the other four cases were fetal rhabdomyomatous nephroblastoma (FRN) or contained a premature skeletal muscle component and appeared to be resistant to chemotherapy because there was no reduction in tumor volume. However, after chemotherapy, most of the tumor components changed into mature striated muscle cells, most of which immunostained almost completely negative for Ki-67. All four cases had the same point mutation of *WT1*. From our results, the histological findings correlated with *WT1* mutations in bilateral WT. The tumor volume of FRN did not decrease in response to chemotherapy. It is possible to predict the chemotherapy response by examining bilateral WT for *WT1* mutations and the histological characteristics of tumors.

Key words: chemotherapy, fetal rhabdomyomatous nephroblastoma, Wilms' tumor, Wilms' tumor suppressor gene

Wilms' tumor (WT) is the most common malignant neoplasm of the kidney in childhood, accounting for approximately 8% of all childhood solid tumors, and 5–10% of WT patients present with bilateral disease.[1,2] Pathologically, bilateral WT tends to be fetal rhabdomyomatous nephroblastoma (FRN), a histological variant of WT characterized by a predominance of rhabdomyogenic components. Clinically, WT of the FRN type presents as a huge mass in younger patients. The tumor rarely metastasizes or shows aggressive behavior, and it has a good prognosis.[3] On the other hand, FRN is known to be resistant to the chemotherapy used to treat classical WT.[4,5] The Wilms' tumor suppressor gene (*WT1*) at chromosome 11p13 was identified in 1990, and it encodes a transcriptional factor containing a domain of four zinc finger motifs.[6,7] Schumacher *et al.* reported finding *WT1* mutations in four of the five cases of bilateral WT that they analyzed,[8] a much higher incidence than in sporadic WT.[1,2] Bilateral WT is explained by the two-hit mechanism of inactivation of tumor suppressor genes proposed by Knudson and Strong.[8–10] Because a germ line mutation in *WT1* has been reported to predispose the development of tumors with stromal-predominant histology,[8] the *WT1* mutation should be found in bilateral WT, especially the FRN histological subtype. However, there have been no reports discussing correlations between the histology of WT, the chemotherapy response and *WT1* mutations.

This report summarizes the clinical and pathological features in five cases of bilateral WT. This study analyzed the *WT1* gene mutation and attempted to determine why they are resistant to chemotherapy.

MATERIALS AND METHODS

Patients

Five patients with bilateral WT who underwent surgery between 1998 and 2001 were studied. Cases 2–5 were accompanied by genitourinary tract malformations (Table 1).

Correspondence: Jun-ichi Hata, MD, National Research Institute for Child Health and Development, 3-35-31 Taishido, Setagaya-ku, Tokyo 154-8567, Japan. Email: jhata@nch.go.jp

Received 19 September 2002. Accepted for publication 6 December 2002.

Table 1 Clinical and histological features and results of *WT1* mutations

Case	Age/Sex	Anomaly	Histology before chemotherapy	First chemotherapy	Tumor volume after therapy	Histological subtype after chemotherapy	Mutations germ line	Mutations tumor	Outcome
1	9 months/F	–	Epithelial type	V+A	Decrease	Epithelial type	–	–	Disease-free postoperative status
2	11 months/M	Cryptorchidism	FRN	V+A+D†	Increase	FRN	1168C→C/T	1168X→T(R390X)	Disease-free postoperative status
3	9 months/F	Cryptorchidism hypospadias	Nephroblastic-type striated muscle (+)	V+A†	Regression (–)	FRN	1168C→C/T	1168X→T(R390X)	Disease-free postoperative status
4	7 months/F	Ovarian dysgenesis	FRN	V+A†	Increase	FRN	1168C→C/T	1168X→T(R390X)	Disease-free postoperative status
5	1 year/M	Cryptorchidism	Nephroblastic-type striated muscle (+)	V+A†	Increase	Nephroblastic-type striated muslce cells: increase	1168C→C/T	1168X→T(R390X)	Under treatment

†Additional aggressive chemotherapy was performed. A, actinomycin; C, cytosine; D, doxorubicin; FRN, fetal rhabdomyomatous nephroblastoma; T, thymine; V, vincristine.

Cases 2 and 5 were associated with cryptorchidism, case 3 with bilateral cryptorchidism and hypospadias, and case 4 with left ovarian dysgenesis. None of the patients showed evidence of renal dysfunction or renal failure. Fresh tumor tissue and peripheral blood samples were obtained from all five patients when tumorectomy was performed. The clinical features of the patients are summarized in Table 1. Informed consent was obtained from all patients or their parents.

Histopathological analysis

The biopsy specimens before chemotherapy and the resected tumors after chemotherapy were fixed with 10% formalin and embedded in paraffin. Paraffin sections were stained with H&E. Histological subtyping of WT was performed according to the classification proposed by the Japanese Society of Pathology, [11] and FRN was defined as more than 1/3 of the tumor mass showing striated muscle differentiation. However, the nephroblastic type of tumor was defined as the tumor that showed triphasic histology containing striated muscle, but its proportion of the tumor was less than 1/3.[11] We used biopsied specimens to diagnose the histology of tumors before chemotherapy. All five cases underwent open biopsy and we took them to represent the histology of tumor. Some sections were subjected to immunohistochemistry for WT1, Ki-67, myogenin and S-100 protein by the avidin-biotin-peroxidase technique using anti-WT1 antibody (dilution 1:200; DAKO, Carpinteria, CA, USA), anti-Ki-67 antibody (dilution 1:500; DAKO, Kyoto, Japan), antimyogenin antibody (dilution 1:200; Santa Cruz, CA, USA) and anti-S-100 protein antibody (dilution 1:2000; DAKO, Japan). For WT1 staining, deparaffinized and rehydrated sections were treated with 0.4% pepsin in 0.2 NHCl for 30 min at 37°C before reacting with anti-WT1 antibody. Deparaffinized and rehydrated sections were heated at 100°C in 0.01 mol/L sodium citrate buffer (pH 6.0) for 10 min before reacting with anti-Ki-67 and antimyogenin antibody.

DNA preparation

The DNA was extracted from leukocytes and tumor tissue by the sodium dodecyl sulfate-proteinase K method with slight modifications, as described previously.[12] Amplification of exons 1–10 was performed by polymerase chain reaction (PCR). Direct sequencing of the PCR products was performed with a MegaBACE 1000 DNA Sequencing System (Amersham Biosciences, Florida, USA). The precise methods have been described previously.[12] The PCR and sequence primers we used are shown in Table 2. All procedures were approved by the Ethical Committee of the Keio University School of Medicine.

Table 2 Polymerase chain reaction (PCR) and sequence primers

exon	Name	PCR sequence	Name	Sequence
1	WT256	AGCCAGAGCAGCAGGGAGTC	SEQ1-S	GGCATCTGGGCCAAGTTAGG
	WTEX1R2	CGGTCAAAAGGGGTAGGAGA	SEQ1-A	CCTAGAGCGGAGAGTCCCTG
2	2B-S	TGGCTGGTTCAGACCCACTG	SEQ2-S	TGCCCCGTCTTGCGAGAGCA
	2B-A	AGAGGAGGATAGCACGGAAG	SEQ2-A	GCACGGAAGAAGGGGAGAAG
3	3B-S	CCAGGCTCAGGATCTCGTGT	SEQ3-S	ATCTCGTGTCTCCCCCAACC
	3B-A	GGCGTCTCGTGCCTCCAAGA	SEQ3-A	GTGCCTCCAACACCCTGCAT
4	4B-S	TGTGGAGGCTTGCACTTTCA	SEQ4-S	GAAGAAACAGTTGTGTATTATTTTG
	4B-A	GCCCTTTCTTCTAAAACTGT	SEQ4-A	ATGGTTCAAACAGGTATAAGTTACT
5	5B-S	TCACTGGATTCTGGGATCTG	SEQ5-S	CTGGGATCTGGGGGGCTTGCCA
	5B-A	AGTCCTAACTCCTGCATTGC	SEQ5-A	CCCCAGGTGCCAGTCAGCAAGG
6	6B-S	AAAACCATCATTCCCTCCTG	SEQ6-S	TTTCCAAATGGCGACTGTGAGC
	6B-A	CAAAGAGTCCATCAGTAAGG	SEQ6-A	GGTAAGTAGGAAGAGGCAGTGC
7	7F-S	GTGCTCACTCTCCCTCAAGA	SEQ7-S	TCCCTCAAGACCTACGTGAATGTTC
	7F-A	GTGAGAGCCTGGAAAAGGAGC	SEQ7-A	TTGAACCATGTTTGCCCAAGACTGG
8	8-S	AGATCCCCTTTTCCAGTATC	SEQ8-S	AGATCCCCTTTTCCAGTATC
	8C'-A	CAACAACAAAGAGAATCA	SEQ8-A	AAATCAACCCTAGCCCAAGG
9	9C-S	AAGTCAGCCTTGTGGGCCTC	SEQ9-S	CCCACATTGGTTAGGGCCGAGGCTA
	9C-A	TTTCCAATCCCCTCTCATCAC	SEQ9-A	TAGGGCCGAGGCTAGACCTTCTCT
10	10C-S	CACTCGGGCCTTGATAGTTG	SEQ10-S	TTTCCAATCCCCTCTCATCAC
	10C-A	GTCAGACTTGAAAGCAGTTC	SEQ10-A	TGTGCCTGTCTCTTTGTTGC

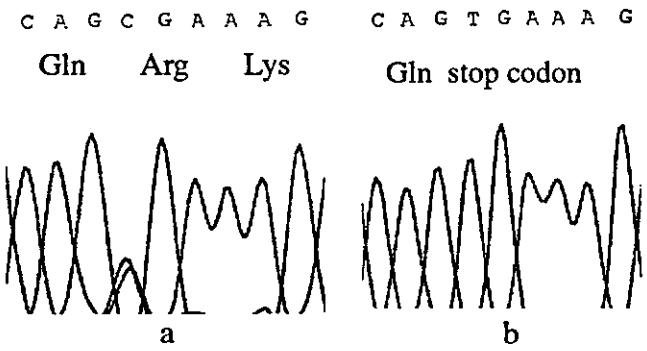

Figure 1 Results of the DNA sequence analyses of germ line (**a**) and tumor samples (**b**). (**a**) A heterozygous point mutation, 1168 cytosine/thymine, was found in exon 9 in the germ line in cases 2–5. (**b**) A point mutation, 1168C/T, converts the codon for 390Arg into a stop codon in the tumors in cases 2–5.

RESULTS

The clinical and pathological features and results of *WT1* mutations are summarized in Table 1. The DNA sequence analyses indicated the same point mutations at exon 9 in cases 2–5. The mutation was a cytosine to a thymine substitution in zing finger 3 and resulted in a ^{390}Arg becoming a stop codon (R390X). There was a heterozygous mutation at the same codon in the germ line of all four patients (Fig. 1). No *WT1* mutation was detected in case 1.

The histological subtype in case 1 was the epithelial type, and the specimens before chemotherapy contained no clear striated muscle components. Cases 2 and 4 showed the typical histological features of FRN. Cases 3 and 5 were nephroblastic type and contained abundant striated muscle components before chemotherapy.

Only case 1 was responsive to chemotherapy consisting of vincristine and actinomycin D. As the tumor volume in the other cases either increased (cases 2, 4, and 5) or was unchanged (case 3), additional aggressive chemotherapy was carried out in these four cases, but tumor regression did not occur regardless of the chemotherapy regimen. Finally, all patients underwent bilateral tumorectomy. Cases 1–4 are disease-free after tumorectomy. In case 5, tumor rupture occurred during chemotherapy, and the patient is now on chemotherapy after bilateral nephrectomy.

Histological examination of all resected tumors after chemotherapy, except in case 1, showed a predominance of mature striated muscle and collagenous tissue (Fig. 2). The epithelial and blastemal components of cases 2–5 were markedly reduced in the tumor tissue. However, we diagnosed case 3 as nephroblastic type before chemotherapy because almost the entire tumor was composed of striated muscle components after chemotherapy. Therefore, we diagnosed case 3 as an FRN-like tumor after chemotherapy. The resected tumor of case 1 contained no striated muscle or collagen fibers. None of the tumors examined showed histological anaplasia before or after chemotherapy.

Before chemotherapy, the striated muscle cells were positive for myogenin, a protein that regulates the differentiatin of myogenic cells and is expressed in the cells induced to differentiate (Fig. 3a), and they were negative for S-100 protein, which is expressed in mature skeletal muscles (Fig. 3b). After chemotherapy, mature striated muscle was negative for myogenin (Fig. 3c) and positive for S-100 protein (Fig. 3d). Ki-67 was positive in the nuclei of almost all of the tumor cells

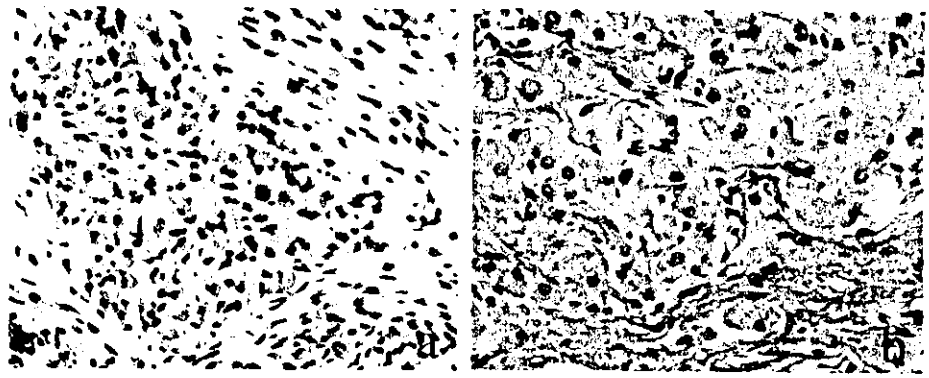

Figure 2 H&E section from case 4. (a) Preoperative biopsy. Immature striated muscle is the predominant stromal element. (original magnification, ×100) (b) Resected tumor after chemotherapy. The components are mostly mature striated muscle and collagen fiber. (original magnification, ×100)

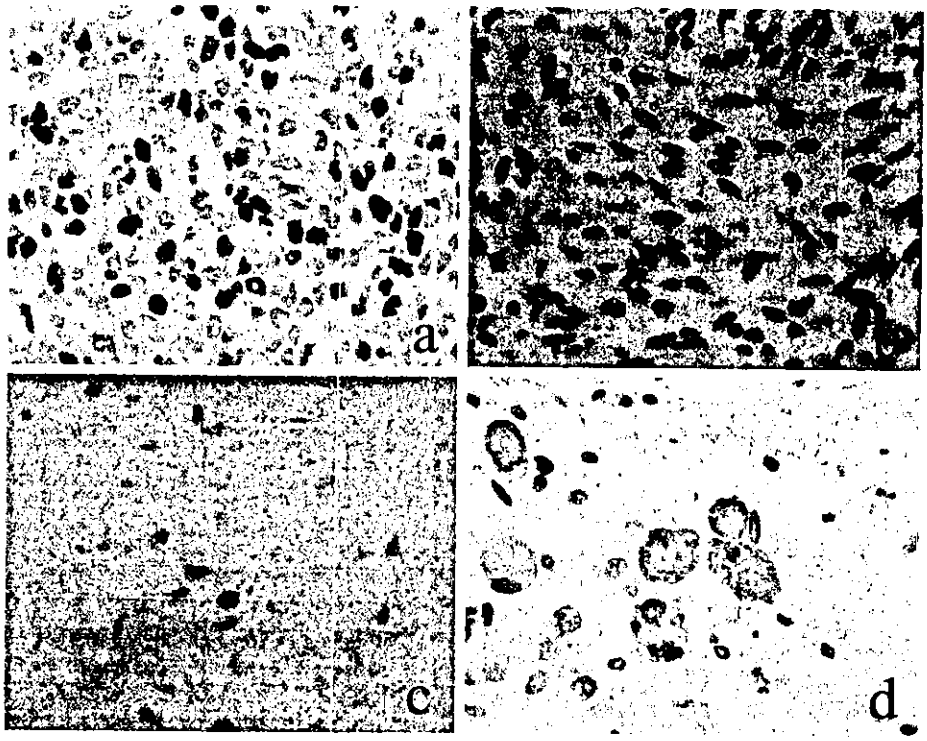

Figure 3 Immunohistochemical analysis of sections from case 4 with myogenin and S-100 protein (original magnification, ×200) (a) Striated muscle cells before chemotherapy are positive for myogenin, a protein that regulates myogeninc cell differentiation and is expressed in cells induced to differentiate. (b) Tumor cells before chemotherapy are negative for S-100 protein, expressed in mature skeletal muscle. (c) Striated muscle cells after chemotherapy are negative for myogenin. (d) Striated muscle cells after chemotherapy are positive for S-100 protein.

before chemotherapy (Fig. 4a), but the mature striated muscle cell components were almost negative for Ki-67 (Fig. 4b). The epithelial and blastemal components of the tumors were positive for Ki-67 (data not shown). The tumors in cases 2–5 that carried the *WT1* point mutation were negative for *WT1* staining (Fig. 5a), whereas case 1, which did not have the *WT1* mutation, was positive for immunostaining (Fig. 5c).

DISCUSSION

In this report, we have summarized the clinical course and histological features in five cases of bilateral WT before and after chemotherapy. We also demonstrated a *WT1* mutation in them. Our results support that loss of *WT1* expression as a result of *WT1* mutation is correlated with the histological features of WT.[8] They also suggest that histological features are related to the response of chemotherapy. As unilateral WTs are usually resected before chemotherapy according to the Japan Wilms' Study Group protocol, it is difficult to compare histological features before and after chemotherapy. The estimated incidence of *WT1* mutation in unilateral or sporadic WT cases is approximately 10–15%.[2] We consider it important to clarify the histological features and response to chemotherapy in bilateral WTs carrying *WT1* mutations with higher incidence than unilateral WTs.

Cases 2–5 were found to have the same point mutations, a change from C to T in zing finger 3, resulting in ^{390}Arg becoming a stop codon. During translation, this nonsense mutation leads to protein truncation, with the result that the last zing finger necessary for DNA binding of *WT1* is missing. Interrupted DNA binding to the target genes of *WT1* fusion

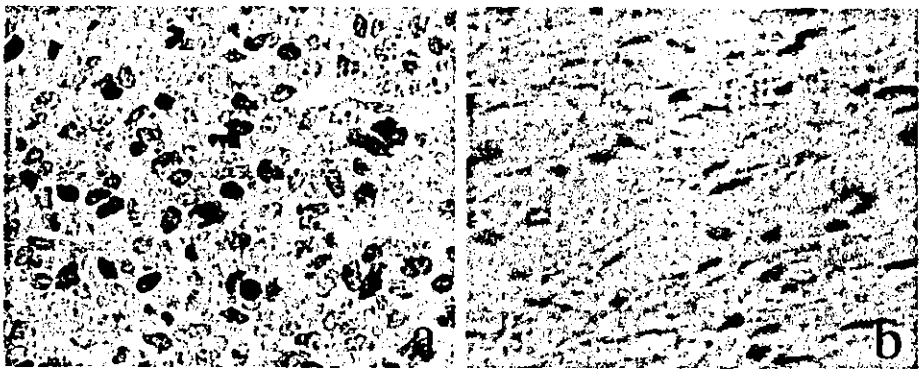

Figure 4 Immunohistochemical analysis of Ki-67 (original magnification, ×400) (**a**) Preoperative biopsy of Case 3. Tumor cells are positive for Ki-67 before chemotherapy. (**b**) Resected tumor of case 3. Tumor tissue is negative for Ki-67.

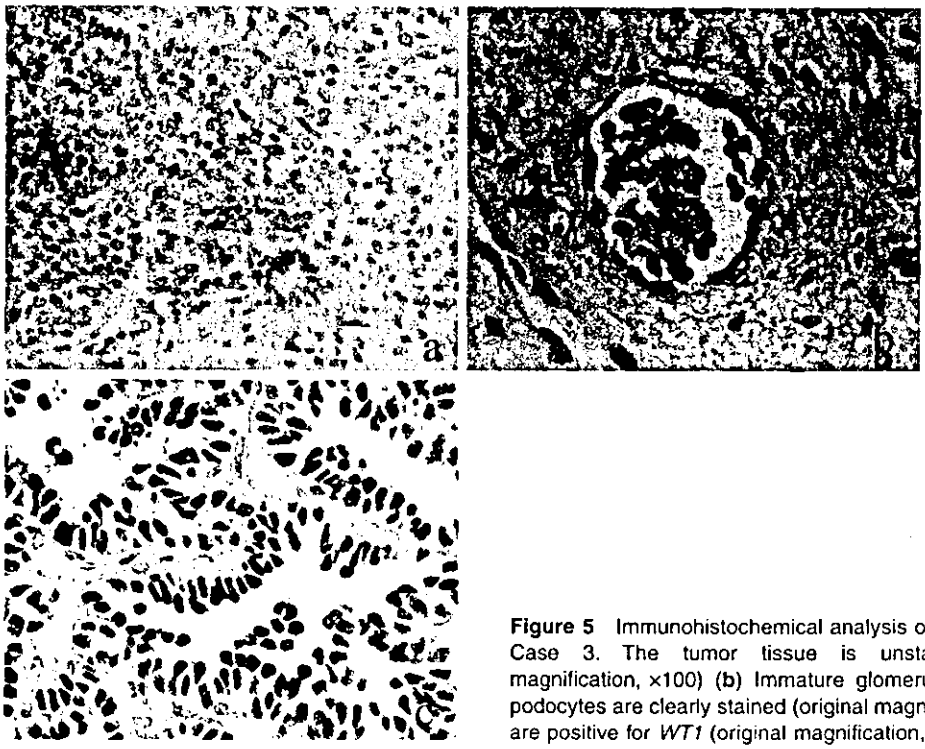

Figure 5 Immunohistochemical analysis of Wilms' tumor suppressor gene (*WT1*). (**a**) Case 3. The tumor tissue is unstained by anti-*WT1* antibody (original magnification, ×100) (**b**) Immature glomerulus in the same section of case 3. The podocytes are clearly stained (original magnification, ×400) (**c**). Case 1. The tumor cells are positive for *WT1* (original magnification, ×400).

proteins with loss of the last zing finger have been previously demonstrated by electrophoretic mobility shift assays.[13] There was a heterozygous mutation at the same point in the germ line of all four patients, thereby supporting the two-hit mutational model of bilateral WT.

In earlier studies, mutation R390X had been found in patients with sporadic unilateral WT, in a patient with bilateral WT, and in a patient with WT associated with urogenital malformation.[14] This mutation has also been detected in a patient with acute promylocytic leukemia[15] and a patient with an isolated genital malformation without WT.[16] Although the histological findings in the WTs with the R390X mutation were not described in the literature, from our results, this R390X mutation might correlate with rhabdomyomatous histology in bilateral WT.

The cases with *WT1* mutation immunohistochemically stained negative for WT1. Loss of *WT1* function has been reported to be the underlying cause of tumor development.[8] Miyagawa *et al.* reported that loss of *WT1* function leads to ectopic myogenesis in WT, and suggested that normal expression of WT1 might prevent the metanephric-mesenchymal stem cells of the kidney from differentiating into skeletal muscle.[17] All four cases had *WT1* mutations, and cases 2 and 4 showed stromal-predominant histology. Cases 3 and 5 showed the nephroblastic type before chemotherapy, and it could not be concluded that all WTs with the R390X mutation present with FRN histologically. Cases 3 and 5 contained skeletal muscle cells as a stromal component. After chemotherapy, case 3 showed FRN and case 5 had more striated muscle cells than before chemotherapy. All

four cases were negative for *WT1*. Loss of *WT1* expression is related to histological features, at least in bilateral WT.

Tumor volume, except for case 1, increased or failed to regress after the usual chemotherapy for classical WT, and the tumors appeared to be resistant to the usual chemotherapy. Histologically, all tumors, except case 1, showed a marked predominance of mature striated muscle, including increased collagen fibers and decreased epithelial and blastemal components, after chemotherapy. Before chemotherapy, all tumor components, stromal, epithelial, and blastemic, were strongly positive for Ki-67, a cell proliferation-related antigen absent in the G0 phase. After chemotherapy,striated muscle, which was the main component of the tumors, was negative for Ki-67. Tubular structures and blastema were positive for Ki-67, but they were a very small component of the tumors. Further, FRN been reported to be a poor responder to preoperative chemotherapy,[4,5] and Anderson *et al.* reported that rhabdomyomatous histology in bilateral Wilms' tumors is associated with poor response to chemotherapy.[18] Except for case 1, tumor volume in either increased or failed to regress after chemotherapy. Histologically, however, the immature component decreased and the mature component increased. The mature component showed less proliferate activity. Apparently, chemotherapy was effective, but tumor volume did not decrease because of the increase in collagen fibers. Most clinicians assume that chemotherapy is ineffective if tumor volume does not change after chemotherapy, and they consider continuous or additional chemotherapy. Additional aggressive chemotherapy consisting of etoposide, carboplatin and cyclophosphamide, which is said to be effective against proliferating tumor cells, was performed in our cases. These anticancer drugs are ineffective against tumors mainly composed of mature striated muscle components. The prognosis of FRN has been said to be good,[3,4] and our four cases have been free of disease since tumor resection. Aggressive chemotherapy, which has little effect on the tumor and might cause complications, should be avoided. The usual chemotherapy for the stage in each side is sufficient. However, there might be residual immature components that show proliferative activity and have the potential to metastasize. Surgical resection of tumors after usual chemotherapy is essential.

Nagashima *et al.* reported myogenic differentiation of stromal cells in the nude mouse WT line.[19] Wilms' tumor tends to spontaneously differentiate into mature elements, although it is not as well known as neuroblastoma. Zuppan *et al.* reported differentiation of WT after preoperative chemotherapy.[20] Seenmayer *et al.* and Ishikawa *et al.* reported a case of WT in which complete maturation of a pulmonary metastasis was documented after chemotherapy.[21,22] Chemotherapy might induce mesenchymal differentiation in WT and promote tumor maturation. The results clearly indicate that immature stromal components in our cases differentiated into mature striated muscles. This maturation is probably attributable to both the inherent nature of WT to differentiate and the effect of chemotherapy.

The histological diagnosis before therapy is important when deciding the management of bilateral WT. If the diagnosis is FRN, chemotherapy could not be expected to result in tumor reduction. Tumors might be resected in the early course of the therapy, for example, after one course of chemotherapy or before chemotherapy, if renal preservation is possible.

In conclusion, the histological features strongly correlate with *WT1* mutation in bilateral WT. Preoperative diagnostic biopsy is important in bilateral WT because if the pathological subtype of the tumor is FRN or it contains striated muscle, tumor volume reduction cannot be the expected response to chemotherapy, even if chemotherapy is effective. Clarification of the biological characteristics of bilateral WT is required in order to determine the most suitable treatment.

ACKNOWLEDGMENTS

We thank Drs H. Horie (Chiba Children's Hospital), K. Hashizume and Y. Kanamori (University of Tokyo Faculty of Medicine), J. Miyauchi and Y. Tsunematsu (National Center for Child Health and Development), Y. Hayashi (Tohoku University School of Medicine) and Y. Ogawa (Saitama Childrenís Medical Center) for providing samples and clinical data. We thank Mr H. Suzuki for his technical assistance.

This work was supported by a Grant-in-Aid for Scientific Research from the Ministry of Education, Culture, Sports, Science and Technology (11557021, 13470053, 13022264 and 11167274), as well as a Cancer Research Grants from the Ministry of Health, Labor and Welfare (9–14, 10D-1).

REFERENCES

1 Coppes MJ, Pritchard-Jones K. Principles of Wilms' tumor biology. *Urol Clin North Am* 2000; **27**: 423–33.
2 Lee SB, Haber DA. Wilms' tumor and the WT1 gene. *Exp Cell Res* 2001; **264**: 74–99.
3 Wigger HJ. Fetal rhabdomyomatous nephroblastoma-a variant of Wilms' tumor. *Hum Pathol* 1976; **7**: 613–23.
4 Maes P, Delemarre J, de Kraker J, Ninane J. Fetal rhabdomyomatous nephroblastoma: a tumour of good prognosis but resistant to chemotherapy. *Eur J Cancer* 1999; **35**: 1356–60.
5 Saba LM, de Camargo B, Gabriel-Arana M. Experience with six children with fetal rhabdomyomatous nephroblastoma: review of the clinical, biologic, and pathologic features. *Med Pediatr Oncol* 1998; **30**: 152–5.
6 Call KM, Glaser T, Ito CY *et al.* Isolation and characterization of a zinc finger polypeptide gene at the human chromosome 11 Wilms' tumor locus. *Cell* 1990; **60**: 509–20.
7 Gessler M, Poustka A, Cavenee W *et al.* Homozygous deletion in Wilms tumours of a zinc-finger gene identified by chromosome jumping. *Nature* 1990; **343**: 774–8.

8 Schumacher V, Schneider S, Figge A *et al.* Correlation of germline mutations and two-hit inactivation of the WT1 gene with Wilms tumors of stromal-predominant histology. *Proc Natl Acad Sci USA* 1997; **94**: 3972–7.
9 Huff V, Miwa H, Haber DA *et al.* Evidence for WT1 as a Wilms tumor (WT) gene: intragenic germinal deletion in bilateral WT. *Am J Hum Genet* 1991; **48**: 997–1003.
10 Knudson AG Jr, Strong LC. Mutation and cancer: a model for Wilms' tumor of the kidney. *J Natl Cancer Inst* 1972; **48**: 313–24.
11 Committee on histological classification of childhood tumors the Japanese pathological society. Histological classification and atlas of tumors in infancy and childhood I T Tumors of the urinary system. In: Urano Y, ed. *Tumors of the Kidneys.* Tokyo: Kanehara, 1988; 12–3.
12 Takata A, Kikuchi H, Fukuzawa R, Ito S, Honda M, Hata J. Constitutional WT1 correlate with clinical features in children with progressive nephropathy. *J Med Genet* 2000; **37**: 698–701.
13 Little M, Holmes G, Bickmore W, van Heyningen V, Hastie N, Wainwright B. DNA binding capacity of the WT1 protein is abolished by Denys–Drash syndrome WT1 point mutations. *Hum Mol Genet* 1995; **4**: 351–8.
14 Little M, Wells C. A clinical overview of WT1 gene mutations. *Hum Mutat* 1997; **9**: 209–25.
15 King-Underwood L, Renshaw J, Pritchard-Jones K. Mutations In the Wilms' tumor gene WT1 in leukemias. *Blood* 1996; **87**: 2171–9.
16 Kohler B, Schumacher V, l'Allemand D, Royer-Pokora B, Grutters A. Germline Wilms tumor suppressor gene (WT1) mutation leading to isolated genital malformation without Wilms tumor or nephropathy. *J Pediatr* 2001; **138**: 421–4.
17 Miyagawa K, Kent J, Moore A *et al.* Loss of WT1 function leads to ectopic myogenesis in Wilms' tumour. *Nat Genet* 1998; **18**: 15–7.
18 Anderson J, Slater O, McHigh K, Duffy P, Pritchard J. Response without shrinkage in bilateral Wilms tumors: Significance of rhabdomyomatous histology. *J Pediatr Hematol Oncol* 2002; **24**: 31–4.
19 Nagashima Y, Nishihira H, Miyagi Y *et al.* A nude mouse Wilms' tumor line (KCMC-WT-1) derived from an aniridia patient with monoalleleic partial deletion of chromosome 11p. *Cancer* 1996; **77**: 799–804.
20 Zuppan CW, Beckwith JB, Weeks DA, Luckey DW, Pringle KC. The effect of preoperative therapy on the histologic features of Wilms' tumor. An analysis of cases from the Third National Wilms' Tumor Study. *Cancer* 1991; **68**: 385–94.
21 Seemayer TA, Harper JL, Shickell D *et al.* Cytodifferentiation of a Wilms' tumor pulmonary metastasis: theoretic and clinical implications. *Cancer* 1997; **79**: 1629–34.
22 Ishikawa K, Toyoda Y, Fukuzato Y, Kato K, Ijiri R, Tanaka Y. Maturation in the primary and metastatic lesions of fetal rhabdomyomatous nephroblastoma. *Med Pediatr Oncol* 2001; **37**: 62–3.